CHAPTER 5 - POLARIZABILITIES AND HYPERPOLARIZABILITIES OF THE BROMOMETHANES

5.1 INTRODUCTION

The electric properties of the halogenomethanes have attracted considerable interest. Buckingham and Orr[1] measured the Kerr effects of methane and its four fluorinated derivatives as vapours at a wavelength of 632.8 nm. Their analysis of the results, which involved effectively the same bond additivity approximation to estimate γ^K for fluoromethane, difluoromethane and trifluoromethane as was used in Chapter 3 for methylamine and dimethylamine, yielded the polarizabilities and the Kerr first and second hyperpolarizabilities of the fluoromethanes. An analogous investigation by Bogaard et al.[2] yielded the polarizabilities and the Kerr first and second hyperpolarizabilities of the chloromethanes. A similar study of the bromomethanes is obviously desirable.

Several studies of the Kerr effects of the brominated derivatives of methane have been reported. Burnham et al.[3] measured the Kerr constant and Rayleigh depolarization ratio of bromomethane as a vapour at a wavelength of 488 nm. Although the lack of a temperature-dependence study precluded the extraction of β^K and γ^K, these quantities were reported to make only a small contribution to the Kerr constant. Le Fèvre and Ritchie[4] measured the molar Kerr constant of tribromomethane as a solute in benzene solution, at 298 K and a wavelength of 589 nm, but neglected the contribution of the hyperpolarizabilities. Karna et al.[5] measured the first hyperpolarizability of bromomethane using electric field-induced second harmonic generation, and also cited a value for the second hyperpolarizability from degenerate four-wave mixing experiments. Izsák and Le Fèvre[6] measured the Kerr constant of dibromomethane in the solution phase, and their results were subsequently reanalyzed by Buckingham and Orr[7] to estimate the Kerr first hyperpolarizability of this species.

Therefore, although the electric properties of several of the bromomethanes have been reported, there have been no systematic investigations of the series. Analysis of the Kerr effects of the four brominated derivatives of methane, similar to the analyses performed for the fluorinated[1] and chlorinated[2] derivatives, would constitute a comprehensive study of halogen substitution. The instability of the carbon - iodine bond under the conditions of the Kerr-effect measurements prevents an analogous investigation of the iodomethanes. Stankey[8] found that iodoethane readily decomposed in the original Kerr cell.

5.2 EXPERIMENTAL

A sample of bromomethane (Matheson, 99.5%) was found by gas chromatography to have a purity of ≥ 99.4% and was used without further purification. A sample of dibromomethane (Aldrich, 99%) was purified by shaking successively with concentrated sulfuric acid, distilled water, a 0.1M sodium hydroxide solution and then once more with distilled water. The sample was then dried over anhydrous calcium chloride for 12 hr and distilled over phosphorous pentoxide. The purified dibromomethane was stored in a brown bottle, over Linde Type 4A molecular sieves, away from bright light. Decomposition of the dibromomethane in the gas-chromatography column prevented its purity being measured.

A sample of tribromomethane (Aldrich, ≥ 99%) was used without further purification. Attempts to remove the ethanol stabiliser by distillation resulted in the immediate decomposition of the sample, even in the dark. The contribution of the ethanol to the observed Kerr effect of tribromomethane was assumed to be negligible, as the original sample contained less than 1% of the more volatile ethanol and the Kerr constants of ethanol in benzene and carbon tetrachloride solutions[9,10] have been shown to be smaller than that of tribromomethane at the same temperature, reported in this work.

The sample of tetrabromomethane (BDH, > 98%) was sublimed twice at 415 K before use. Tetrabromomethane is a solid at room temperature and pressure (mp 363 K), while dibromomethane and tribromomethane are liquids (bp 370 K and 423 K, respectively) and bromomethane is a gas (bp 277 K). This chapter presents the first reported investigation of the vapour-phase Kerr effects of a series of compounds with these three physical states under normal conditions.

Density second virial coefficients are available for bromomethane for the temperature range 287.8 - 321.1 K [11] At higher temperatures, the necessary values were calculated using the Stockmayer potential.[12] No virial coefficients were available for dibromomethane. As the critical temperature, pressure and volume and the Antoine coefficients are also unknown for this species, the coefficients calculated for dichloromethane,[13] using the method of Pitzer,[14] were used. Any error due to this assumption is minimised by the low gas densities used for dibromomethane. Similarly, the virial coefficients of tribromomethane and tetrabromomethane appear to be unknown and, in light of the low gas densities used, these were assumed to be zero. Furthermore, the low volatilities of these two compounds prevented investigation of the density dependences of their Kerr effects. Therefore, the values of A_K reported for tribromomethane and tetrabromomethane were taken to be equal to the weighted averages of the measured Kerr constants at that temperature, and no values of B_K are reported. This approximation is reasonable, as the statistical uncertainties of the measured Kerr constants of these two compounds were significantly larger than the effects of any realistic density dependence. Due to the instability of tetrabromomethane, few measurements were possible on this compound before obvious decomposition occurred. The Kerr virial coefficients measured for bromomethane, dibromomethane, tribromomethane and tetrabromomethane in the vapour phase are listed in Tables 5.1, 5.2, 5.3 and 5.4, respectively.

Table 5.1 Kerr effect of bromomethane at 632.8 nm

T / K	Number of Pressures	Pressure Range / kPa	$10^6 B$ a) / m^3 mol^{-1}	$10^{27} A_K$ / C^2 m^5 J^{-2} mol^{-1}	$10^{29} B_K$ b) / C^2 m^8 J^{-2} mol^{-2}
295.0	10	35 - 106	−597	89.94 ± 0.09	−3.0 ± 0.3
306.3	10	34 - 107	−548	83.26 ± 0.06	−1.1 ± 0.2
318.8	11	39 - 112	−495	77.13 ± 0.07	−0.5 ± 0.2
332.2	10	40 - 114	−438	72.78 ± 0.12	−3.9 ± 0.3
347.3	11	40 - 118	−387	66.26 ± 0.34	−4 ± 1
365.6	11	38 - 111	−336	59.13 ± 0.07	1.0 ± 0.3
386.7	9	34 - 111	−290	53.74 ± 0.06	−1.3 ± 0.2
414.6	11	37 - 114	−244	47.54 ± 0.06	−2.7 ± 0.2
444.7	9	37 - 111	−206	41.33 ± 0.09	−0.7 ± 0.4
470.6	10	39 - 121	−181	37.21 ± 0.14	−1.6 ± 0.5
495.1	10	41 - 122	−161	33.82 ± 0.05	−0.7 ± 0.3

a) Density second virial coefficients from reference 11 and calculated values (see text). b) Calculated using $10^{40} \alpha$ / C^2 m^2 J^{-1} = 6.22 ± 0.06, from reference 15, $10^{40} \alpha^0$ / C^2 m^2 J^{-1} = 6.48 ± 0.18, from reference 16, and $10^{30} \mu$ / C m = 6.0768 ± 0.0012, from reference 17.

Table 5.2 Kerr effect of dibromomethane at 632.8 nm

T / K	Number of Pressures	Pressure Range / kPa	$10^6 B$ a) / $m^3\ mol^{-1}$	$10^{27} A_K$ / $C^2\ m^5\ J^{-2}\ mol^{-1}$	$10^{29} B_K$ b) / $C^2\ m^8\ J^{-2}\ mol^{-2}$
360.1	10	27 - 59	−533	−15.51 ± 0.05	−2.4 ± 0.3
364.0	10	23 - 55	−521	−15.30 ± 0.21	14 ± 1
378.9	11	26 - 63	−475	−13.72 ± 0.04	1.5 ± 0.3
385.2	10	27 - 66	−459	−12.67 ± 0.05	3.9 ± 0.3
405.5	9	25 - 55	−406	−11.47 ± 0.10	3 ± 1
429.0	9	26 - 57	−359	−9.80 ± 0.05	2.4 ± 0.3
439.2	10	33 - 71	−341	−9.04 ± 0.07	2.0 ± 0.5
454.2	9	31 - 70	−316	−7.97 ± 0.07	1.1 ± 0.5
465.8	10	28 - 59	−298	−6.75 ± 0.07	−3 ± 1
476.4	9	34 - 77	−283	−6.52 ± 0.09	−0.3 ± 0.6
500.2	9	39 - 84	−253	−5.42 ± 0.09	0.2 ± 0.5

a) Density second virial coefficients from reference 13. b) Calculated using $10^{40}\alpha / C^2\ m^2\ J^{-1} = 9.61 \pm 0.10$, from reference 18, $10^{40}\alpha^0 / C^2\ m^2\ J^{-1} = 10.10 \pm 0.35$, from reference 16, and $10^{30}\mu / C\ m = 4.74 \pm 0.07$, from reference 16.

Table 5.3 Kerr effect of tribromomethane at 632.8 nm

T / K	Pressure / kPa	$10^{27} A_K$ / $C^2 m^5 J^{-2} mol^{-1}$
354.6	9.5	−15.8 ± 0.8
367.4	15.2	−14.91 ± 0.16
374.2	17.3	−13.63 ± 0.06
382.1	18.7	−12.69 ± 0.08
387.8	14.9	−11.99 ± 0.13
393.1	19.2	−11.70 ± 0.07
405.5	14.1	−9.96 ± 0.20
413.8	22.3	−9.30 ± 0.04
433.8	20.4	−8.05 ± 0.21

Table 5.4 Kerr effect of tetrabromomethane at 632.8 nm

T / K	Pressure / kPa	$10^{27} A_K$ / $C^2 m^5 J^{-2} mol^{-1}$
384.6	3.65	2.2 ± 1.0

5.3 DISCUSSION

The temperature dependences of the Kerr effects of the bromomethanes are shown in Figure 5.1. There is an obvious contrast between the positive sign and curvature of the results for bromomethane, shown in the top graph, and those of dibromomethane and tribromomethane, in the lower graph. The results for dibromomethane are represented by the circles and unbroken curve and those of tribromomethane by the triangles and dashed curve. For bromomethane at 298 K and a wavelength of 488.0 nm, Burnham et al.[3] measured ${}_{\mathrm{m}}K = (91.6 \pm 2.8) \times 10^{-27}\ \mathrm{C^2\ m^5\ J^{-2}\ mol^{-1}}$, which is in good agreement with the value of $A_{\mathrm{K}} = 88.3 \times 10^{-27}\ \mathrm{C^2\ m^5\ J^{-2}\ mol^{-1}}$ extrapolated from this work at the same temperature and 632.8 nm. The precision of this result is much higher than that of the earlier value, as shown by the small statistical uncertainties of the values of A_{K} in Table 5.1. Dispersion is likely to account for some of the discrepancy between these two values.

Le Fèvre and Ritchie[4] reported an infinite-dilution molar Kerr constant for tribromomethane of ${}_{\infty}({}_{\mathrm{m}}K_2) = -37.6 \times 10^{-27}\ \mathrm{C^2\ m^5\ J^{-2}\ mol^{-1}}$ at 298 K and 589 nm, in benzene. Extrapolation of the results presented here gives the admittedly uncertain, yet undoubtedly smaller, value of $A_{\mathrm{K}} \approx -27 \times 10^{-27}\ \mathrm{C^2\ m^5\ J^{-2}\ mol^{-1}}$ at 632.8 nm for tribromomethane as a free molecule. The large discrepancy between these two values is presumably due to the strong dipole-quadrupole, and other solute-solvent, interactions between the tribromomethane and benzene molecules in the solution-phase measurements. For similar reasons, there are also differences between the reported Kerr constants of dibromomethane. Izsák and Le Fèvre[6] found, from solution-phase Kerr-effect measurements on dibromomethane at 298 K and 589 nm, that in carbon tetrachloride ${}_{\infty}({}_{\mathrm{m}}K_2) = -19.6 \times 10^{-27}\ \mathrm{C^2\ m^5\ J^{-2}\ mol^{-1}}$, and in benzene ${}_{\infty}({}_{\mathrm{m}}K_2) = -26.3 \times 10^{-27}\ \mathrm{C^2\ m^5\ J^{-2}\ mol^{-1}}$ A value of $A_{\mathrm{K}} = -23.2 \times 10^{-27}\ \mathrm{C^2\ m^5\ J^{-2}\ mol^{-1}}$ at 632.8 nm and the same temperature is obtained by extrapolation of the results in this work.

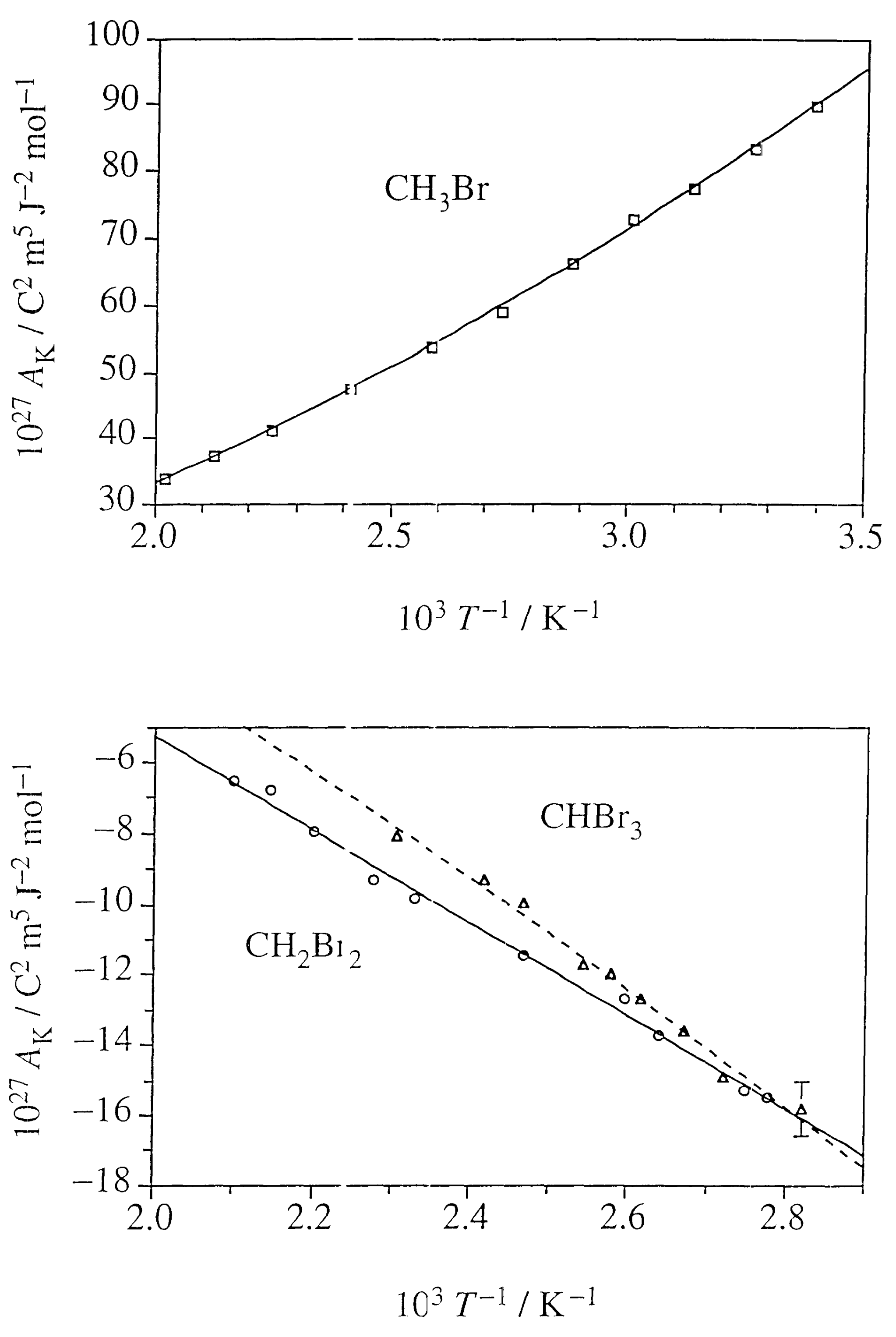

Figure 5.1 The Kerr effects of the bromomethanes.

The temperature dependences of the Kerr effects of the bromomethanes were analyzed in a similar manner to that discussed in previous chapters. Depolarization ratios obtained from Rayleigh light-scattering experiments by Keir[19] at 632.8 nm were combined with mean polarizabilities, derived from refractive indices at the same wavelength, to determine the polarizabilities of both bromomethane and tribromomethane. Carocci et al.[17] have measured the dipole moments of both $CH_3{}^{79}Br$ and $CH_3{}^{81}Br$, using Stark spectroscopy. The dipole moment of CH_3Br was taken as the average over the isotopic distributions[20] ($CH_3{}^{79}Br$: $CH_3{}^{81}Br$ = 50.54% : 49.46%). As no microwave spectroscopy experiments have been performed on dibromomethane or tribromomethane, the dipole moments of both molecules were obtained from the vapour-state dielectric polarization measurements by Buckingham and Le Fèvre.[16] Mean static polarizabilities for bromomethane, dibromomethane and tribromomethane were also obtained from this reference. The Kerr first and second hyperpolarizabilities of bromomethane and tribromomethane were then determined from the equation

$$\begin{aligned}\left\{A_{\mathrm{K}} - \left(N_{\mathrm{A}}/270\varepsilon_0 k^2\right)\mu^2(\alpha_{zz} - \alpha)T^{-2}\right\} &= (N_{\mathrm{A}}/81\varepsilon_0)\gamma^{\mathrm{K}} + \\ &\quad (N_{\mathrm{A}}/81\varepsilon_0 k)\left\{(2/3)\mu\beta^{\mathrm{K}} + (9/5)\alpha\alpha^0\kappa\kappa^0\right\}T^{-1}\end{aligned} \tag{5.1}$$

as depicted in Figures 5.2 and 5.3. For bromomethane, the quantity being plotted against T^{-1} is only a small percentage of A_{K}, as shown by a comparison of these values with those in Table 5.1. This makes the scatter of the data points from the line of best fit more pronounced. Despite this, the gradient of the line in Figure 5.2 is reasonably well defined.

The results for dibromomethane were analyzed in an analogous manner to those of methylamine and dimethylamine in Chapter 3. That is, the Kerr second hyperpolarizability of dibromomethane was interpolated from a weighted fit of the corresponding values for methane,[1] bromomethane, tribromomethane and tetrabromomethane. The Kerr first hyperpolarizability and the quantity $\alpha_{zz} - \alpha$ were then determined from the equation

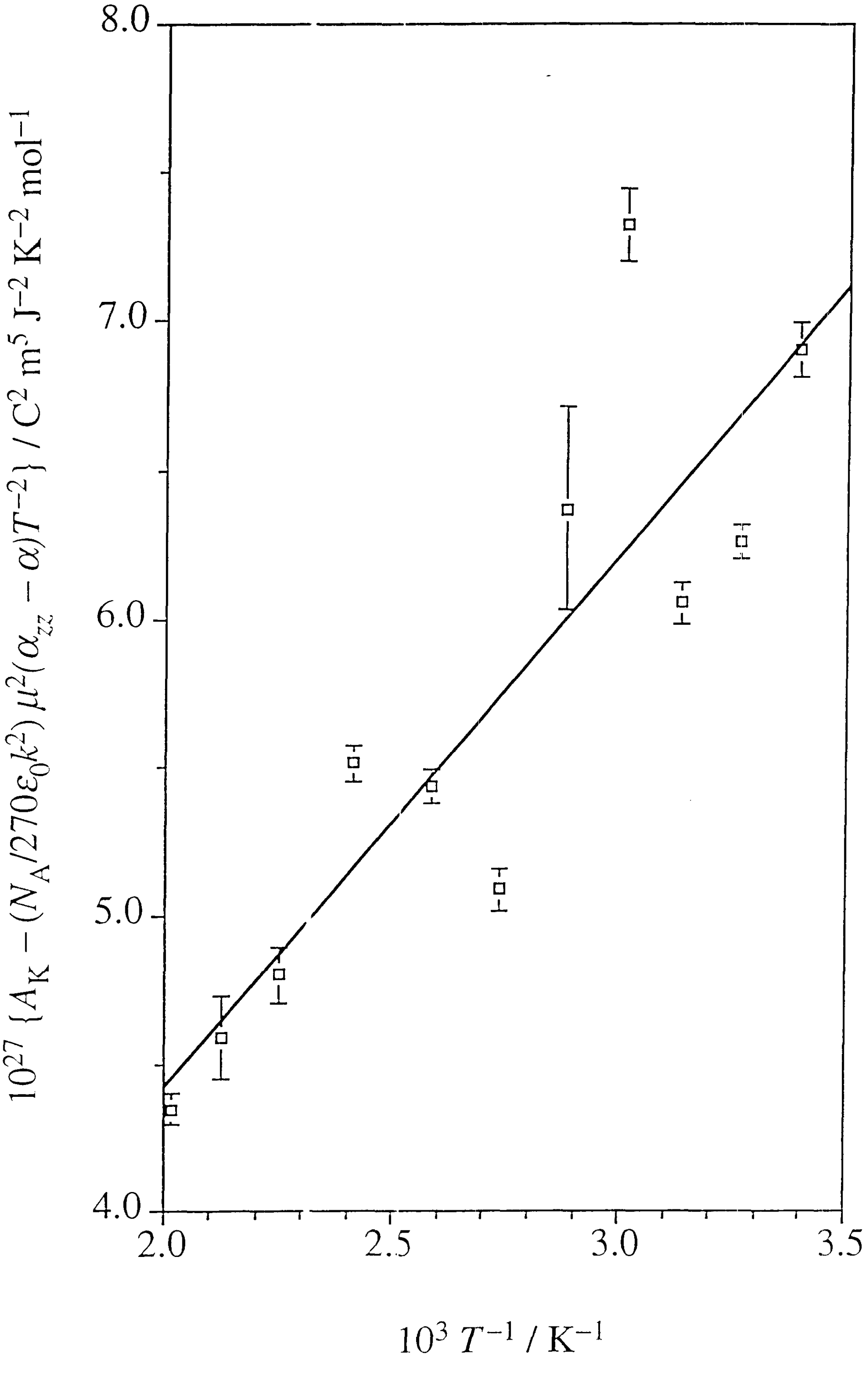

Figure 5.2 Analysis of the Kerr effect of bromomethane.

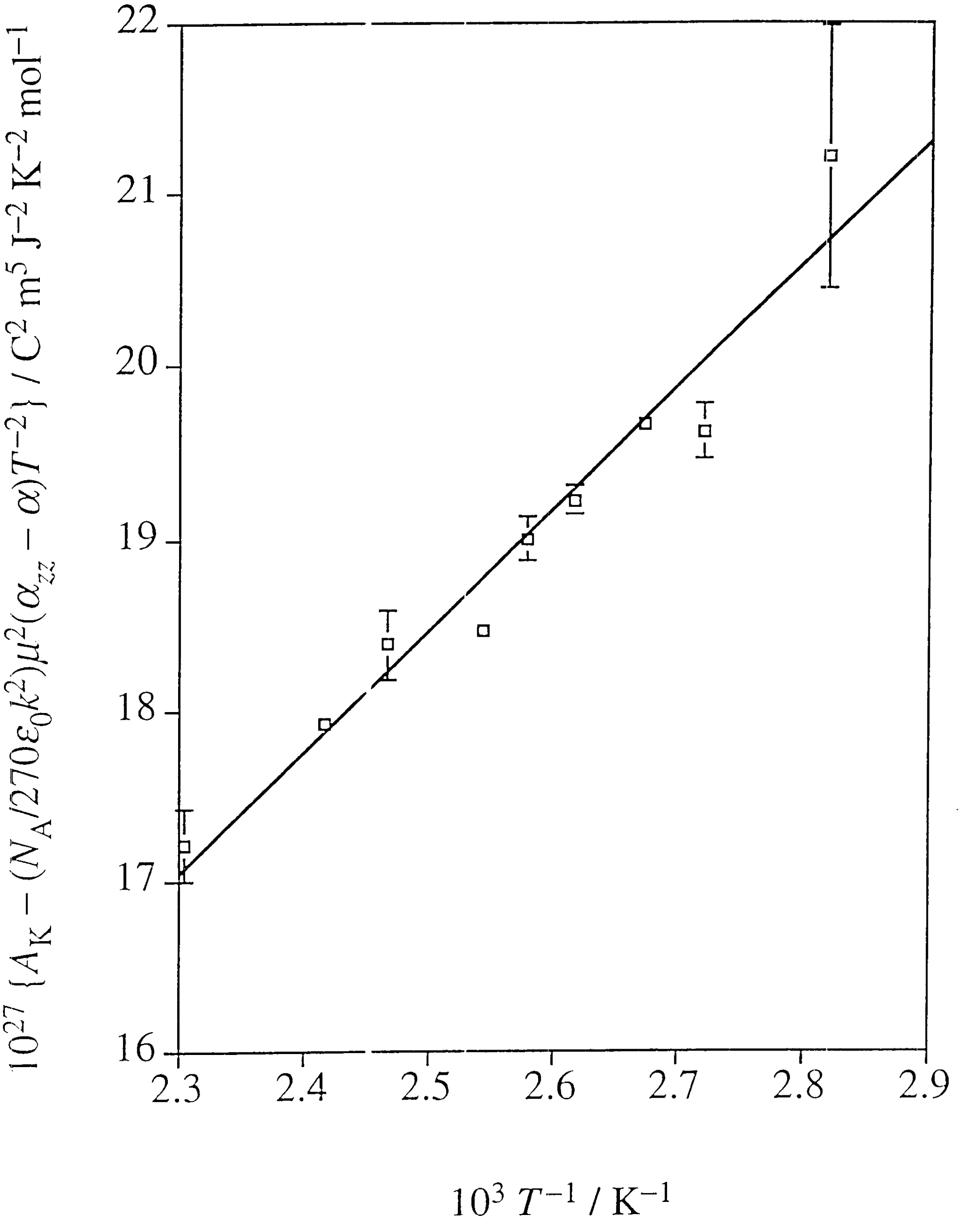

Figure 5.3 Analysis of the Kerr effect of tribromomethane.

$$\left[A_K - (N_A/81\varepsilon_0)\gamma^K\right]T = (N_A/81\varepsilon_0 k)\left\{\left[(2/3)\mu\beta^K + (9/5)\alpha\alpha^0\kappa^2\right] + (3/10k)\mu^2(\alpha_{zz} - \alpha)T^{-1}\right\} \tag{5.2}$$

as depicted in Figure 5.4. The Kerr second hyperpolarizability of tetrabromomethane is related to A_K by equation 1.14. Tables 5.5, 5.6 and 5.7 list the derived electric properties of bromomethane, dibromomethane and tribromomethane, respectively.

The Kerr second hyperpolarizability of tetrabromomethane at 632.8 nm was measured to be $\gamma^K = (2.6 \pm 1.2) \times 10^{-60}\ C^4\ m^4\ J^{-3}$. No other value for the second hyperpolarizability of tetrabromomethane has been reported. Figure 5.5 shows that, within the experimental errors, the Kerr second hyperpolarizabilities of methane,[1] bromomethane, tribromomethane and tetrabromomethane are additive and increase regularly with bromine substitution, despite the experimental difficulties encountered during these measurements. Therefore, the interpolated value of γ^K for dibromomethane should be reasonably accurate. A comparison with the measured Kerr second hyperpolarizabilities of tetrafluoromethane[1] and tetrachloromethane[2] indicates that γ^K also increases as the size of the halogen atom increases.

Similarly distinct trends are not observed for the Kerr first hyperpolarizabilities of the bromomethanes, possibly for the reason that the experimental observable transforms as a vector. This absence of additivity with substitution was also found for the fluoromethanes[1] and chloromethanes,[2] as shown in Table 5.8. As with the Kerr second hyperpolarizabilities, a comparison of the β^K values for the three halogenomethane series indicates that, in general, the magnitude of β^K increases with fluorine to chlorine to bromine substitution. However, the Kerr first hyperpolarizabilities of the bromomethanes are all of the same sign, unlike those of the fluoromethanes and the chloromethanes. The reasons for, and significance of, this are not clear, although the uncertainties associated with the Kerr first hyperpolarizabilities of the chloromethanes suggest that their signs are ambiguous.

The present study yields the first reliable value of the Kerr first hyperpolarizability of dibromomethane, $\beta^K = (0.4 \pm 0.2) \times 10^{-50}\ C^3\ m^3\ J^{-2}$. Buckingham and Orr[7]

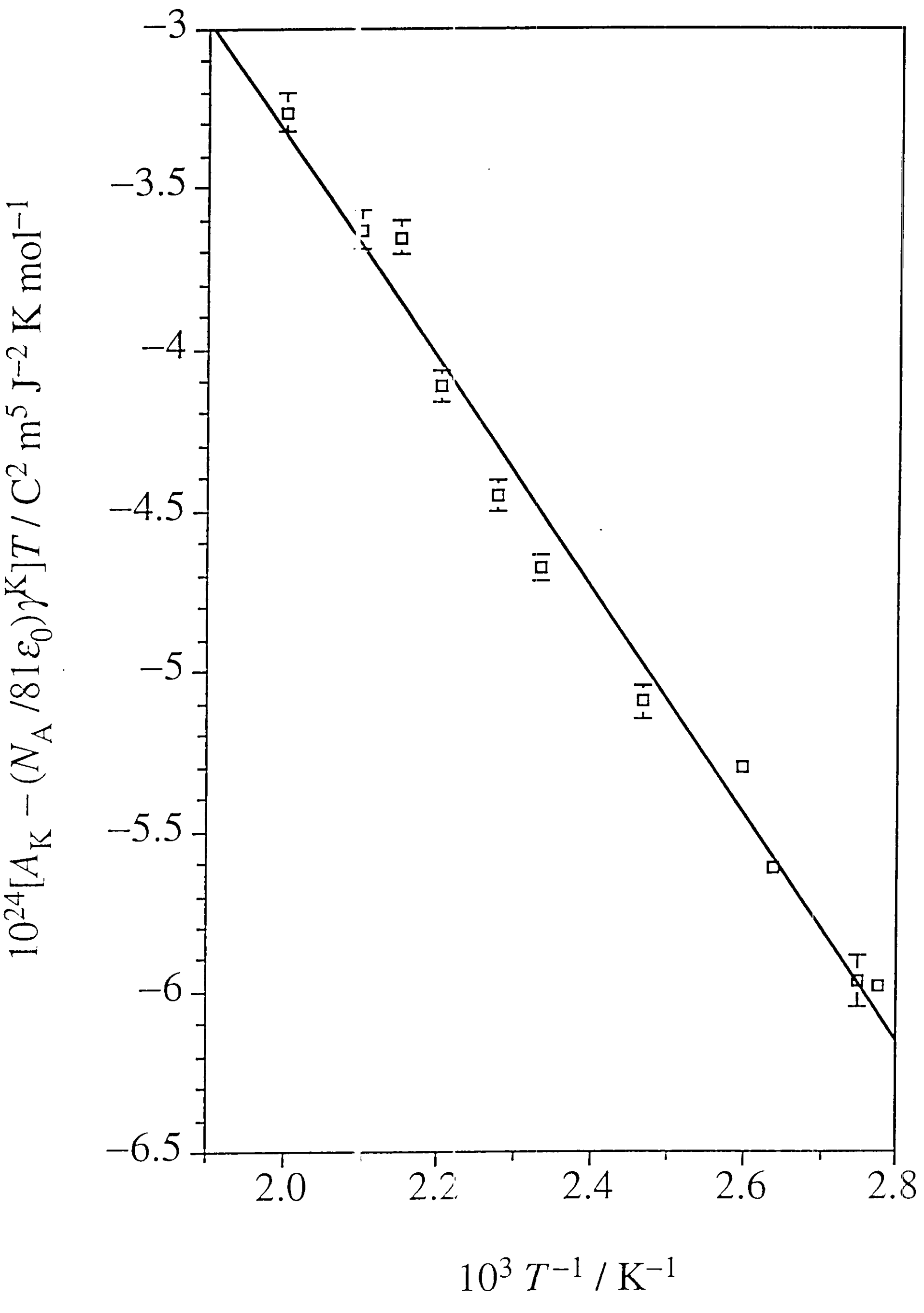

Figure 5.4 Analysis of the Kerr effect of dibromomethane.

Table 5.5 Analysis of the Kerr effect of bromomethane at 632.8 nm

Property	Value
10^{24} slope / C^2 m^5 J^{-2} K^{-1} mol^{-1} a)	1.79 ± 0.34
10^{27} intercept / C^2 m^5 J^{-2} K^{-2} mol^{-1} a)	0.8 ± 0.9
10^{40} α / C^2 m^2 J^{-1} b	6.22 ± 0.06
10^{40} α^0 / C^2 m^2 J^{-1} c)	6.48 ± 0.18
10^2 κ^2 d)	1.416 ± 0.005
10^{30} μ / C m e)	6.0768 ± 0.0012
10^{40} α_{xx} / C^2 m^2 J^{-1}	5.48 ± 0.06
10^{40} α_{yy} / C^2 m^2 J^{-1}	5.48 ± 0.06
10^{40} α_{zz} / C^2 m^2 J^{-1}	7.70 ± 0.07
10^{50} β^K / C^3 m^3 J^{-2}	0.5 ± 0.1
10^{60} γ^K / C^4 m^4 J^{-3}	1.0 ± 1.1

a) From equation 5.1. b) Reference 15. c) Reference 16. d) Reference 19.

e) Reference 17.

Table 5.6 Analysis of the Kerr effect of dibromomethane at 632.8 nm

Property	Value
10^{21} slope / $C^2\ m^5\ J^{-2}\ K^2\ mol^{-1}$ a)	-3.43 ± 0.15
10^{24} intercept / $C^2\ m^5\ J^{-2}\ K\ mol^{-1}$ a)	3.49 ± 0.38
$10^{40}\ \alpha$ / $C^2\ m^2\ J^{-1}$ b	9.61 ± 0.10
$10^{40}\ \alpha^0$ / $C^2\ m^2\ J^{-1}$ c)	10.10 ± 0.35
$10^2\ \kappa^2$ d)	2.539 ± 0.029
$10^{30}\ \mu$ / C m c)	4.74 ± 0.07
$10^{60}\ \gamma^K$ / $C^4\ m^4\ J^{-3}$	1.6
$10^{40}\ (\alpha_{zz} - \alpha)$ / $C^2\ m^2\ J^{-1}$	-1.16 ± 0.05
$10^{40}\ \alpha_{xx}$ / $C^2\ m^2\ J^{-1}$	12.64 ± 0.14
$10^{40}\ \alpha_{yy}$ / $C^2\ m^2\ J^{-1}$	7.73 ± 0.18
$10^{40}\ \alpha_{zz}$ / $C^2\ m^2\ J^{-1}$	8.45 ± 0.11
$10^{50}\ \beta^K$ / $C^3\ m^3\ J^{-2}$	0.4 ± 0.2

a) From equation 5.2. b) Reference 18. c) Reference 16. d) Reference 19.

Table 5.7 Analysis of the Kerr effect of tribromomethane at 632.8 nm

Property	Value
10^{24} slope / $C^2\ m^5\ J^{-2}\ K^{-1}\ mol^{-1}$ a)	6.4 ± 0.4
10^{27} intercept / $C^2\ m^5\ J^{-2}\ K^{-2}\ mol^{-1}$ a)	2.3 ± 1.1
$10^{40}\ \alpha$ / $C^2\ m^2\ J^{-1}$ b	13.02 ± 0.26
$10^{40}\ \alpha^0$ / $C^2\ m^2\ J^{-1}$ c)	13.1 ± 0.9
$10^2\ \kappa^2$ d)	1.54 ± 0.04
$10^{30}\ \mu$ / C m c)	3.30 ± 0.07
$10^{40}\ \alpha_{xx}$ / $C^2\ m^2\ J^{-1}$	14.64 ± 0.26
$10^{40}\ \alpha_{yy}$ / $C^2\ m^2\ J^{-1}$	14.64 ± 0.26
$10^{40}\ \alpha_{zz}$ / $C^2\ m^2\ J^{-1}$	9.79 ± 0.29
$10^{50}\ \beta^K$ / $C^3\ m^3\ J^{-2}$	2.7 ± 0.4
$10^{60}\ \gamma^K$ / $C^4\ m^4\ J^{-3}$	2.8 ± 1.3

a) From equation 5.1. b) Reference 21. c) Reference 16. d) Reference 19.

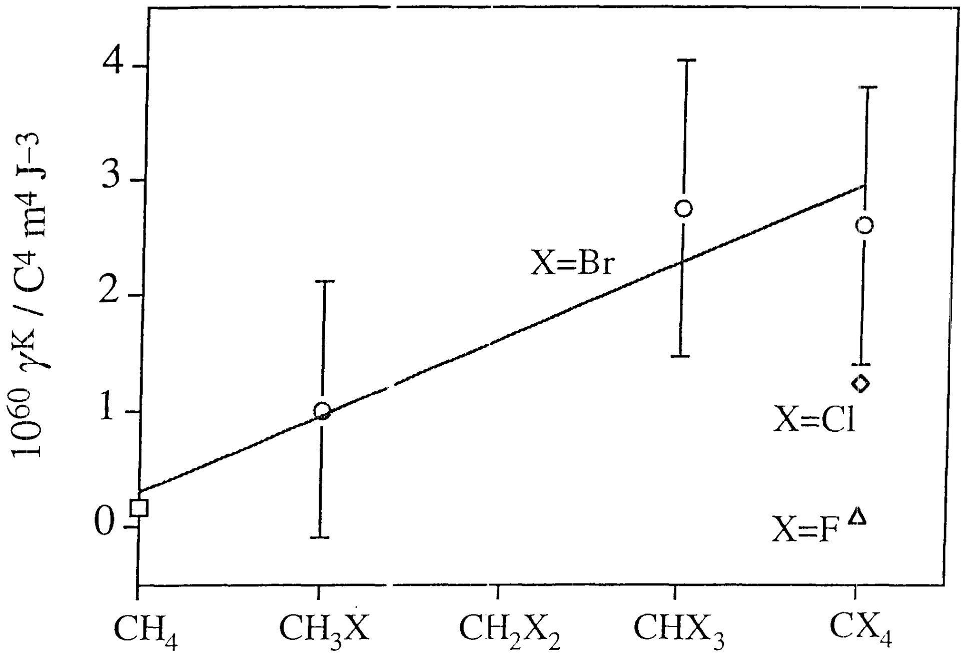

Figure 5.5 Kerr second hyperpolarizabilities of the halogenomethanes from measurements in the vapour phase.

Table 5.8 Measured Kerr first hyperpolarizabilities of the halogenomethanes in the vapour phase a)

	CH_3X	CH_2X_2	CHX_3
X = F b)	−0.19 ± 0.15	−0.03 ± 0.05	0.3 ± 0.2
X = Cl c)	−0.1 ± 0.4	0.4 ± 0.5	−0.5 ± 0.4
X = Br	0.5 ± 0.1	0.4 ± 0.2	2.7 ± 0.4

a) Expressed in units of $10^{-50}\ C^3\ m^3\ J^{-2}$. b) References 1 and 21. c) Reference 2.

estimated values of β^{K} which are an order of magnitude larger than this, from a reanalysis of the solution-phase measurements by Izsák and Le Fèvre.[6] However, the authors noted that their values were uncertain and may be unreliable by up to an order of magnitude. No other values of the first and second hyperpolarizabilities of dibromomethane have been reported for any nonlinear optical process. In the analysis of their single-temperature Kerr constant for bromomethane, Burnham et al.[3] cited an electric field-induced second harmonic generation measurement for bromomethane, at an unknown wavelength. These values of $\beta(-2\omega;\omega,\omega) = 0.17\times10^{-50}\,\mathrm{C^3\,m^3\,J^{-2}}$ and $\gamma(-2\omega;0,\omega,\omega) = 0.42\times10^{-60}\,\mathrm{C^4\,m^4\,J^{-3}}$ are smaller than, but of the same order of magnitude as, the Kerr hyperpolarizabilities measured in this work. There have also been only two previously reported values for the hyperpolarizabilities of tribromomethane, both being cited by Karna et al.[5] The value of $\gamma(-\omega;\omega,\omega,-\omega) = 3.0\times10^{-60}\,\mathrm{C^4\,m^4\,J^{-3}}$, obtained from degenerate four-wave mixing measurements at 602 nm in tetrahydrofuran solutions, is similar to the value of $\gamma^{\mathrm{K}} = (2.8\pm1.3)\times10^{-60}\,\mathrm{C^4\,m^4\,J^{-3}}$ measured in this work. A large disparity is also noted between the Kerr first hyperpolarizability at 632.8 nm, $\beta^{\mathrm{K}} = (2.7\pm0.4)\times10^{-50}\,\mathrm{C^3\,m^3\,J^{-2}}$, and a liquid-phase measurement of $\beta(-2\omega;\omega,\omega) = 0.45\times10^{-50}\,\mathrm{C^3\,m^3\,J^{-2}}$, at 1064 nm.[5,22] This discrepancy does not appear unreasonable when the differences in the physical states of the samples and the dispersion and vibrational contributions to the hyperpolarizabilities of each nonlinear optical process are considered.

The orientations of the molecular axes of the bromomethanes are shown in Figure 5.6, with the y - axis for each molecule being perpendicular to the page. This study has yielded the first experimentally determined set of polarizabilities for dibromomethane, presented in Table 5.6. The mean polarizability of this species at 632.8 nm was interpolated from liquid-phase refractive index measurements.[18] The magnitudes of the polarizabilities for dibromomethane follow the same trend as observed for difluoromethane[1] and dichloromethane,[2] in the order $\alpha_{xx} > \alpha_{zz} > \alpha_{yy}$. This was also predicted for dibromomethane by Applequist et al.,[23] who used an atom - dipole

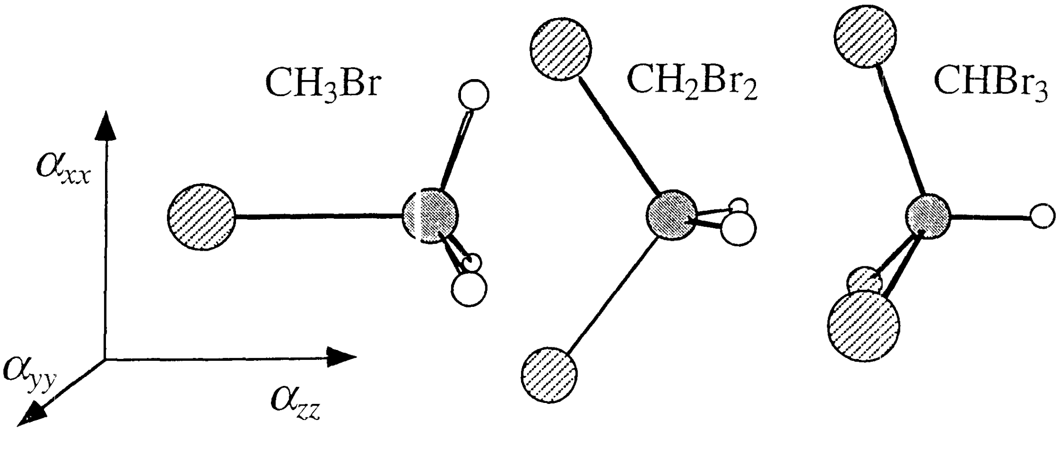

Figure 5.6 Molecular axes of the bromomethanes.

interaction model to estimate $\alpha_{xx} = 14.7$, $\alpha_{yy} = 6.58$ and $\alpha_{zz} = 8.29$ $\times 10^{-40}$ C^2 m^2 J^{-1} at 589 nm. As the authors noted, their model generally exaggerated the polarizability anisotropy, with the differences between calculated and experimental polarizability components often being 10%. Keir[19] has also recently calculated $\alpha_{xx} = 12.86$, $\alpha_{yy} = 7.69$ and $\alpha_{zz} = 8.51 \times 10^{-40}$ C^2 m^2 J^{-1} for dibromomethane at 632.8 nm, at the MP2 level using the HUZI-SV (+sd+sp) basis set.[24] These ab initio values are obviously in good agreement with this work.

Figure 5.7 shows the polarizability components, normalized with respect to the mean polarizability, as a function of halogen substitution for the fluoro-, chloro- and bromo-methanes. The molecular axes for all three series are the same as shown in Figure 5.6. Although α_{zz} makes the largest contribution to the mean polarizability for all three monosubstituted halogeno methanes, this is most pronounced for chloromethane and bromomethane. This contrasts with the trihalogenomethanes, in which the α_{zz} component is coincident with the C-H bond and makes a smaller contribution to the mean polarizability than α_{xx} and α_{yy}. This is again most obvious with the larger chloro- and bromo-methanes. It is evident that, for molecules of formula CH_2X_2, as the halogen atoms increase in size from fluorine to chlorine to bromine, α_{xx} makes a larger contribution to the mean polarizability and α_{yy} and α_{zz} become less significant by

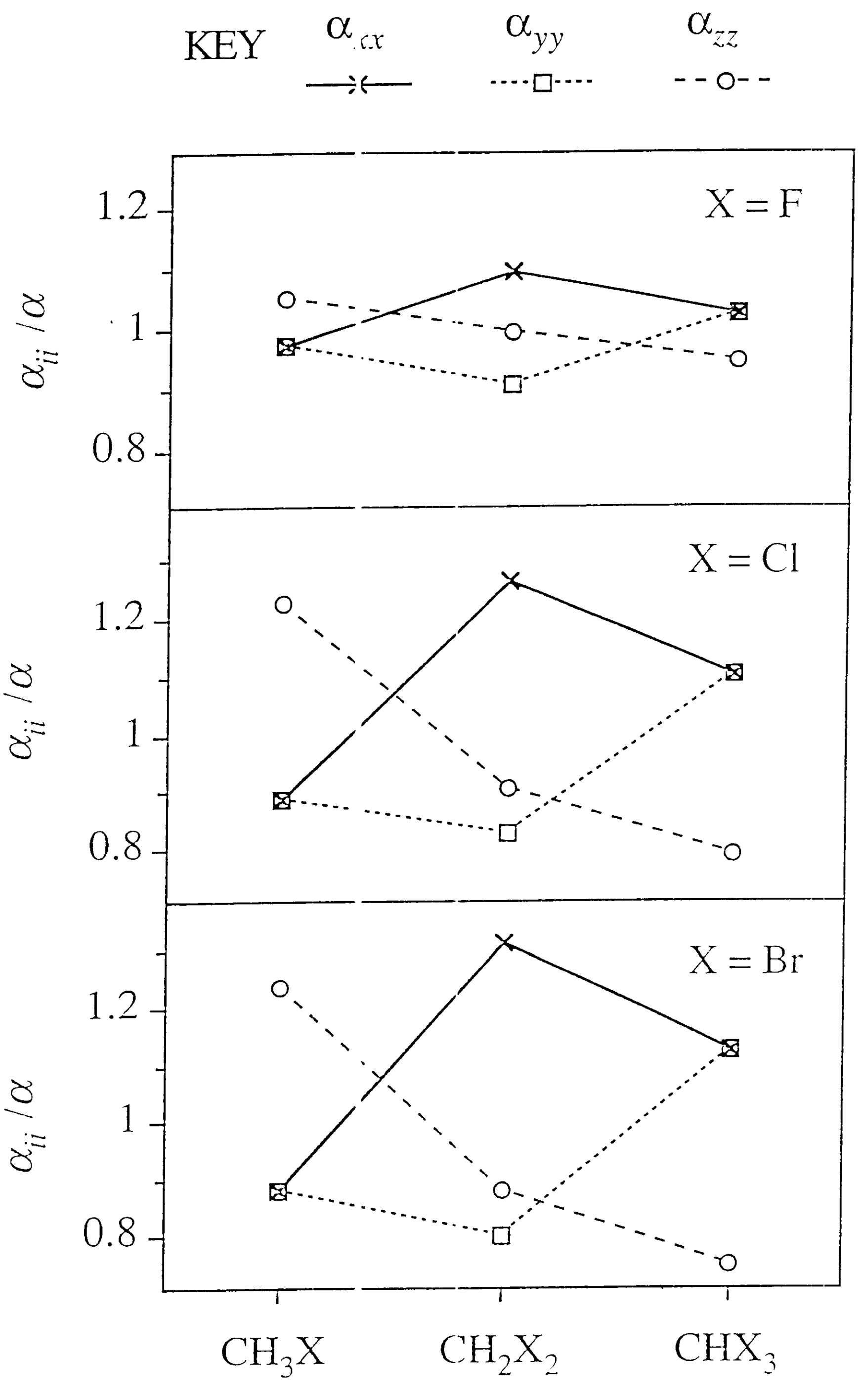

Figure 5.7 Normalized components of the mean polarizabilities of the halogenon ethanes.

approximately the same proportion.

It is of interest to note the very similar relative contributions to the mean polarizability of the polarizability components of the chloro- and bromo- analogues. Although there is a slightly greater anisotropy in the polarizabilities of the bromomethanes than the chloromethanes, the differences are minor. This similarity raises the question of the relative contributions for the iodomethanes. From Rayleigh light-scattering measurements on iodomethane vapour at a wavelength of 488.0 nm, Burnham et al.[3] found that $\alpha_{zz} = 10.64$ and $\alpha_{xx} = \alpha_{yy} = 7.63 \times 10^{-40}\,\mathrm{C^2\,m^2\,J^{-1}}$. Therefore, for iodomethane, $\alpha_{xx}/\alpha = \alpha_{yy}/\alpha = 0.884$ and $\alpha_{zz}/\alpha = 1.232$; results which are almost identical to the values obtained for chloromethane and bromomethane. The free-molecule polarizabilities of diiodomethane and triiodomethane have not been measured, although Le Fèvre and Ritchie[4] have measured the polarizabilities of triiodomethane in the solution phase at 589 nm. However, these latter results are complicated by local-field effects and cannot be compared with this work.

An approximately linear decrease in the α_{zz}/α term is observed with increasing halogen substitution in all three halogenomethanes series. Through the series CH_3X, CH_2X_2, CHX_3 the α_{zz} component is, in turn, oriented along a C-X bond, the bisector of the X-C-X angle and then along a C-H bond. Therefore, in this progression the polarizability of each C-X bond makes a smaller contribution to α_{zz}, while the less polarizable C-H bonds make a larger contribution.

The contributions to the observed Kerr effects of the bromomethanes at 400 K are listed in Table 5.9. This temperature was chosen to provide a point of comparison, as the Kerr first virial coefficients of three of the four bromomethanes were measured spanning this temperature, while A_K for tetrabromomethane is, or is expected to be, independent of temperature. For bromomethane, dibromomethane and tribromomethane the dominant contribution arises from the $\mu^2(\alpha_{zz} - \alpha)$ term, as is generally found for dipolar molecules. Upon successive bromine substitution from bromomethane to tribromomethane, this contribution increases relative to the Kerr first virial coefficient by $\approx 90\%$, to a maximum of 270%, of A_K. This bears an inverse correlation with the

Table 5.9 Contributions of individual terms to A_K for the bromomethanes at 400 K [a)]

Term	CH_3Br	CH_2Br_2	$CHBr_3$	CBr_4
$(N_A/81\varepsilon_0)\gamma^K$	0.8 (1.6%)	1.4 (−11%)	2.3 (−21%)	2.2 (100%)
$(2N_A/243\varepsilon_0 kT)\mu\beta^K$	3.2 (6.2%)	2.0 (−16%)	8.9 (−83%)	–
$(9N_A/405\varepsilon_0 kT)\alpha\alpha^0\kappa^2$	1.6 (3.1%)	6.7 (−57%)	7.2 (−67%)	–
$(N_A/270\varepsilon_0 k^2T^2)\mu^2(\alpha_{zz}-\alpha)$	45.2 (89.4%)	−21.4 (181%)	−29.1 (270%)	–
A_K	50.5	−11.8	−10.7	2.2

a) Expressed in units of 10^{-27} C^2 m^5 J^{-2} mol^{-1}.

decreasing contribution of the α_{zz} term to the mean polarizability. As α_{zz}/α decreases, $\mu^2(\alpha_{zz}-\alpha)$ becomes more negative and makes a larger contribution to the negative Kerr constants of dibromomethane and tribromomethane.

The contributions of the $\mu\beta^K$ and $\alpha\alpha^0\kappa^2$ terms to the Kerr first virial coefficients of bromomethane, dibromomethane and tribromomethane also increase in magnitude, although in a nonlinear manner. Furthermore, these terms make small and positive contributions to A_K for bromomethane, but large and negative contributions for dibromomethane and tribromomethane. The cancellation of the large and oppositely signed contributions of the hyperpolarizability terms results in small Kerr constants for dibromomethane and tribromomethane, as shown in Tables 5.2 and 5.3 and Figure 5.1.

It has already been noted in this chapter that the Kerr second hyperpolarizability is approximately additive with bromine substitution. The γ^{K} term is almost negligible for bromomethane but, as the Kerr first virial coefficients of dibromomethane and tribromomethane are relatively small, the contribution of the γ^{K} term becomes significant with increasing bromine substitution.

Burnham et al.[3] estimated the contributions to the Kerr constant of bromomethane that they measured at 298 K and 488 nm. Their derived contributions are in generally good agreement with the corresponding quantities determined in this work, with the $\mu^2(\alpha_{zz}-\alpha)$ term being dominant and the $\alpha\alpha^0\kappa^2$ term being small. However, the esimated contributions yielded a Kerr constant of ${}_{\mathrm{m}}K = 86.5\times10^{-27}\,\mathrm{C^2\,m^5\,J^{-2}\,mol^{-1}}$, which was smaller than their measured value of ${}_{\mathrm{m}}K = (91.6\pm2.8)\times10^{-27}$ $\mathrm{C^2\,m^5\,J^{-2}\,mol^{-1}}$. As the temperature dependence of the Kerr effect of bromomethane was not investigated by Burnham et al., they could not extract values for the Kerr first and second hyperpolarizabilities. In their analysis, Burnham et al.[3] used first and second hyperpolarizabilities obtained from second harmonic generation measurements. These values of $\beta(-2\omega;\omega,\omega)$ and $\gamma(-2\omega;0,\omega,\omega)$ have already been shown to be smaller than the corresponding values of β^{K} and γ^{K}. The differences between the hyperpolarizabilities measured by means of the Kerr effect and second harmonic generation account for the major part of the difference between the experimental and estimated Kerr constants reported by Burnham et al.

Few conclusions can be drawn about the Kerr second virial coefficients of the bromomethanes from these measurements. There appears to be a contrast between the negative B_{K} values for bromomethane and the positive values for dibromomethane. The imprecision of these results and the inability to apply the collision-induced polarizability model[25] for these molecules, due to the force constants being unknown, prevent a more detailed analysis of the influence of bromine substitution on B_{K}.

5.4 CONCLUSIONS

Despite the reactivity and low volatility of the bromomethanes, the Kerr effects of all four members of this series were measured as vapours in order to examine the effect of bromine substitution on the electric properties. The Kerr second hyperpolarizability was shown to be approximately additive with bromine substitution, and the polarizabilities of dibromomethane were obtained for the first time. A comparison of the electric properties of the bromomethanes with those of the fluoromethanes and chloromethanes illustrated the effects of halogen substitution on the polarizability tensor, the Kerr first and second hyperpolarizabilities and the various contributions to the observed Kerr constants. The results for bromomethane were shown to be in good agreement with, and yet more reliable than, those of an earlier study.

5.5 REFERENCES

1 Buckingham, A.D. and Orr, B.J., *Trans. Faraday Soc.*, **65**, 673 (1969).

2 Bogaard, M.P., Orr, B.J., Buckingham, A.D. and Ritchie, G.L.D., *J. Chem. Soc., Faraday Trans. 2*, **74**, 573 (1978).

3 Burnham, A.K., Buxton, L.W. and Flygare, W.H., *J. Chem. Phys.*, **67**, 4990 (1977).

4 Le Fèvre, R.J.W. and Ritchie, G.L.D., *J. Chem. Soc.*, 4933 (1963).

5 Karna, S.P., Dupuis, M., Perrin, E. and Prasad, P.N., *J. Chem. Phys.*, **92**, 7418 (1990).

6 Izsák, D. and Le Fèvre, R.J.W., *J. Chem. Soc. B*, 102 (1966).

7 Buckingham, A.D. and Orr, B.J., *Quart. Rev.*, **21**, 195 (1967).

8 Stankey, R., *M.Sc. Thesis* (University of New England, 1991).

9 Le Fèvre, C.G., Le Fèvre, R J.W., Purnachandra Rao, B. and Williams, A.J., *J. Chem. Soc.*, 123 (1960).

10 Le Fèvre, R.J.W. and Williams, A.J., *J. Chem. Soc.*, 128 (1960).

11 Dymond, J.H. and Smith, E.B., *The Virial Coefficients of Pure Gases and Mixtures* (Clarendon Press, Oxford, 1980).

12 Hirschfelder, J.O., Curtiss, C F. and Bird, R.B., *Molecular Theory of Gases and Liquids* (Wiley, New York, 1964).

13 Keir, R.I., unpublished results.

14 Pitzer, K.S., *J. Am. Chem. Soc.*, **77**, 3427 (1955).

15 Bogaard, M.P., Buckingham, A.D., Pierens, R.K. and White, A.H., *J. Chem. Soc., Faraday Trans. I*, **74**, 3008 (1978).

16 Buckingham, A.D. and Le Fèvre, R.J.W., *J. Chem. Soc.*, **4**, 3432 (1953).

17 Carocci, S., Minguzzi, P., Tonelli, M. and Di Lieto, A., *J. Mol. Spect.*, **160**, 359 (1993).

18 Vogel, A.I., *J. Chem. Soc.*, 1333 (1948).

19 Keir, R.I., *Ph.D. Thesis* (University of New England, 1995).

20 Weast, R.C., *CRC Handbook of Chemistry and Physics*, 48th Edition (The Chemical Rubber Co., Cleveland, 1967).

21 Orr, B.J., *Hyperpolarizabilities of Halogenated Methane Molecules: A Critical Survey* in *Nonlinear Behaviour of Molecules, Atoms and Ions in Electric, Magnetic and Electromagnetic Fields* (L. Néel ed.), (Elsevier, Amsterdam, 1979).

22 Karna, S.P., Perrin, E., Prasad, P.N. and Dupuis, M., *J. Phys. Chem.*, **95**, 4329 (1991).

23 Applequist, J., Carl, J.R. and Kwok-Keung Fung, *J. Am. Chem. Soc.*, **94**, 2952 (1972).

24 Dougherty, J. and Spackman, M.A., *Mol. Phys.*, **82**, 193 (1994).

25 Buckingham, A.D., Galwas, P.A. and Liu Fan-Chen, *J. Mol. Struct.*, **100**, 3 (1983).

CHAPTER 6 - ANISOTROPIC POLARIZABILITIES OF THE FLUOROBENZENES

6.1 INTRODUCTION

There have been relatively few reported studies of the free-molecule electric properties of aromatic compounds. Benzene and the fluorobenzenes are the notable exception. Buckingham, Ritchie and coworkers have measured the polarizabilities and hyperpolarizabilities,[1,2] magnetizabilities[3,4,5] and quadrupole moments[6,7] of benzene and several members of the fluorobenzenes series. In particular, Gentle et al.[1,2] reported the temperature dependences of the Kerr effects of benzene, fluorobenzene, 1,3,5-trifluorobenzene, pentafluorobenzene and hexafluorobenzene. The polarizability anisotropies of these species were determined to a high level of precision, and fluorine substitution was found to have a small, yet consistent, effect on the polarizabilities of the molecules, but a greater influence on the static and optical-frequency polarizability anisotropies of the nondipolar fluorobenzenes. The relationship between these quantities and the Kerr first virial coefficients for nondipolar species with C_{3v} or higher symmetry has been described in Chapter 1.

Aroney et al.[8] have measured the Kerr constants of, and derived apparent principal polarizabilities for, many of the fluorobenzenes in the solution phase. However, the free-molecule polarizabilities of several of these species are still unknown. The main aim of this study was, therefore, to measure the polarizabilities of 1,2-difluorobenzene, 1,3-difluorobenzene and 1,2,3,5-tetrafluorobenzene and to determine the relationship between the static and optical frequency polarizability anisotropies for 1,4-difluorobenzene and 1,2,4,5-tetrafluorobenzene.

Gentle et al.[1,2] have shown that the Kerr second hyperpolarizabilities make only a small contribution to the Kerr constants of the fluorobenzenes they investigated. Therefore, it is also desirable to measure the hyperpolarizabilities of the di- and tetra-fluorobenzenes and to compare them with those of the other members of this series.

6.2 EXPERIMENTAL

The sample of 1,2-difluorobenzene (Aldrich, 98%), distilled twice over phosphorus pentoxide using a fractionating column, was found, by gas chromatography, to have a purity of ≥ 99.7%. Samples of 1,3-difluorobenzene (Aldrich, ≥ 99%) and 1,4-difluorobenzene (Aldrich, ≥ 99%), similarly distilled over phosphorus pentoxide before use, were found to have purities of ≥ 99.3%.

The sample of 1,2,3,5-tetrafluorobenzene (Aldrich, 95%) was refluxed over sodium and phosphorus pentoxide for 5 hr, dried over sodium wire for 12 hr and fractionally distilled twice over sodium and phosphorus pentoxide. The sample of 1,2,4,5-tetrafluorobenzene (Aldrich, ≥ 99%) was dried over phosphorus pentoxide for 5 days, refluxed over phosphorus pentoxide for 1 hr and then fractionally distilled over phosphorus pentoxide. Gas chromatography showed the purities of 1,2,3,5- and 1,2,4,5-tetrafluorobenzene to be ≥ 98.2% and ≥ 99.6%, respectively. Due to the small sizes of the samples of the tetrafluorobenzenes, each had to be redistilled over phosphorus pentoxide and reused twice to complete the Kerr-effect studies reported here. In order to minimize contamination, the gas Kerr cell was cleaned each time before the repurified tetrafluorobenzenes were used. The recycled materials were found by gas chromatography to be less pure by less than 0.1%.

Gas densities for 1,2-difluorobenzene were calculated using tabulated density second virial coefficients[9] for the temperature range 345.9 - 398.8 K. At higher temperatures, virial coefficients were calculated using the Stockmayer potential.[10] No density virial coefficients have been reported for the other di- and tetra-fluorobenzenes. Gentle[11] used the arithmetic means of the coefficients for benzene and hexafluorobenzene to estimate those for 1,3,5-trifluorobenzene. In a similar manner, the coefficients for 1,3- and 1,4-difluorobenzene were taken to be the averages of those for fluorobenzene and 1,3,5-trifluorobenzene; and the virial coefficients for 1,2,3,5- and 1,2,4,5-tetrafluorobenzene were estimated as being the averages of those of 1,3-difluorobenzene and hexafluorobenzene. Due to the low pressures used in these measurements, the maximum deviation from the ideal gas law was less than 1% and any errors in the estimated density virial coefficients will have a negligible effect upon the Kerr virial coefficients.

The mean optical-frequency polarizabilities of the difluorobenzenes were determined from their refractive indices at 632.8 nm.[12] The dispersions in the refractive indices of the tetrafluorobenzenes are unknown, and the mean polarizabilities of these species were determined from their refractive indices at 589 nm.[12] No values of the mean static polarizabilities of any of the di- or tetra-fluorobenzenes have been reported and there is a similar lack of information about the infrared vibrational intensities of these molecules. Gentle[11] assumed that the mean static polarizability of pentafluorobenzene scaled to the mean polarizability at 632.8 nm in the same way as for fluorobenzene. The same procedure was used to estimate the mean static polarizabilities of the di- and tetra-fluorobenzenes, with these values being assigned uncertainties of ± 5%. As the mean static polarizabilities were used only to calculate the Kerr second virial coefficients and Kerr second hyperpolarizabilities, which were already uncertain, this assumption is not serious. Dipole moments for 1,2- and 1,3-difluorobenzene[13] and 1,2,3,5-tetrafluorobenzene[14] were available from microwave spectroscopic measurements.

Tables 6.1, 6.2, 6.3, 6.4 and 6.5 and Figure 6.1 summarize the Kerr-effect results for 1,2-, 1,3- and 1,4-difluorobenzene and 1,2,3,5- and 1,2,4,5-tetrafluorobenzene, respectively. The results for 1,4-difluorobenzene include three data points measured by Gentle,[15] using an earlier version of the apparatus described in Chapter 2; these earlier values of A_K are in excellent agreement with those determined in the present study. In Figure 6.1, the results for 1,3-difluorobenzene are denoted by the squares and solid curve and those of 1,2,3,5-tetrafluorobenzene are shown by the crosses and dashed curve.

The depolarization ratios of 1,2- and 1,3-difluorobenzene were measured by the author, and the results are listed in Table 6.6. These measurements were made at 353 K with vapour pressures of 3.7 - 25.4 kPa for 1,2-difluorobenzene, and 5.3 - 6.5 kPa for 1,3-difluorobenzene. A large number of depolarization ratios were measured for 1,2-

Table 6.1 Kerr effect of 1,2-difluorobenzene at 632.8 nm

T / K	Number of Pressures	Pressure Range / kPa	$10^6 B$ [a] / $m^3\ mol^{-1}$	$10^{27} A_K$ / $C^2\ m^5\ J^{-2}\ mol^{-1}$	$10^{28} B_K$ [b] / $C^2\ m^8\ J^{-2}\ mol^{-2}$
345.9	8	19 - 38	−1418	207.0 ± 0.4	−2.8 ± 0.3
363.5	5	32 - 42	−1226	186.6 ± 2.5	−1 ± 2
380.9	10	21 - 43	−1036	170.6 ± 0.3	−0.9 ± 0.3
398.8	10	23 - 43	−922	159.5 ± 0.4	−3.4 ± 0.4
416.8	9	22 - 38	−812	144.9 ± 0.2	−2.6 ± 0.2
435.1	9	23 - 40	−720	131.7 ± 0.4	−0.6 ± 0.4
453.7	10	23 - 41	−645	120.3 ± 0.3	−0.5 ± 0.3
472.1	10	23 - 42	−581	112.2 ± 0.2	−0.1 ± 0.3
491.0	10	23 - 42	−527	103.3 ± 0.3	0.5 ± 0.4

a) Density second virial coefficients from reference 9 and calculated values (see text). b) Calculated using $10^{40}\alpha / C^2\ m^2\ J^{-1} = 11.52 \pm 0.12$, from reference 12, $10^{40}\alpha^0 / C^2\ m^2\ J^{-1} = 12.6 \pm 0.6$ (assumed value) and $10^{30}\mu / C\ m = 8.64 \pm 0.07$, from reference 13.

Table 6.2 Kerr effect of 1,3-difluorobenzene at 632.8 nm

T / K	Number of Pressures	Pressure Range / kPa	$10^6 B$ a) / $m^3\ mol^{-1}$	$10^{27} A_K$ / $C^2\ m^5\ J^{-2}\ mol^{-1}$	$10^{28} B_K$ b) / $C^2\ m^8\ J^{-2}\ mol^{-2}$
346.3	10	26 - 46	−1229	74.1 ± 0.2	−0.6 ± 0.1
363.5	9	26 - 49	−1088	67.8 ± 0.2	−0.1 ± 0.2
381.0	8	26 - 51	−961	62.5 ± 0.1	−0.6 ± 0.1
402.1	8	33 - 53	−830	55.7 ± 0.1	−0.1 ± 0.1
424.2	10	33 - 69	−717	50.7 ± 0.1	0.1 ± 0.1
450.6	6	35 - 59	−618	44.9 ± 0.1	0.4 ± 0.1
466.6	9	23 - 41	−576	42.3 ± 0.6	0.9 ± 0.7
477.8	9	25 - 40	−554	41.7 ± 0.3	−0.4 ± 0.3
488.2	10	25 - 51	−540	41.4 ± 0.2	−1.5 ± 0.3

a) Estimated density second virial coefficients (see text). b) Calculated using $10^{40}\alpha$ / $C^2\ m^2\ J^{-1}$ = 11.37 ± 0.11, from reference 12, $10^{40}\alpha^0$ / $C^2\ m^2\ J^{-1}$ = 12.4 ± 0.6 (assumed value) and $10^{30}\mu$ / C m = 5.04 ± 0.07, from reference 13.

Table 6.3 Kerr effect of 1,4-difluorobenzene at 632.8 nm

T / K	Number of Pressures	Pressure Range / kPa	$10^6 B$ a) / m^3 mol^{-1}	$10^{27} A_K$ / C^2 m^5 J^{-2} mol^{-1}	$10^{29} B_K$ b) / C^2 m^8 J^{-2} mol^{-2}
350.2	9	25 - 43	−1195	15.4 ± 0.2	−2 ± 2
368.0	10	23 - 48	−1054	14.4 ± 0.1	−0.6 ± 0.7
370.5 c)	7	10 - 78	−1036	14.4 ± 0.1	−0.5 ± 0.2
381.7 c)	6	20 - 77	−958	13.9 ± 0.1	−0.7 ± 0.6
385.5	9	25 - 49	−931	14.3 ± 0.1	−2 ± 1
395.8 c)	5	40 - 81	−869	13.4 ± 0.1	−0.1 ± 0.4
407.9	9	24 - 52	−797	13.2 ± 0.1	−1 ± 1
435.0	9	24 - 46	−672	12.3 ± 0.2	0 ± 2
462.8	8	23 - 50	−584	11.2 ± 0.1	6 ± 1
466.7	9	24 - 53	−575	11.4 ± 0.2	2 ± 2
481.1	7	40 - 58	−549	11.3 ± 0.3	−1 ± 3
490.8	11	33 - 87	−538	11.2 ± 0.1	−0.6 ± 0.6

a) Estimated density second virial coefficients (see text). b) Calculated using $10^{40}\alpha / C^2\,m^2\,J^{-1} = 11.34 \pm 0.23$, from reference 12, and $10^{40}\alpha^0 / C^2\,m^2\,J^{-1} = 12.4 \pm 0.5$ (assumed value). c) Reference 15.

Table 6.4 Kerr effect of 1,2,3,5-tetrafluorobenzene at 632.8 nm

T / K	Number of Pressures	Pressure Range / kPa	$10^6 B$ [a] / m^3 mol^{-1}	$10^{27} A_K$ / C^2 m^5 J^{-2} mol^{-1}	$10^{28} B_K$ [b] / C^2 m^8 J^{-2} mol^{-2}
337.7	9	14 31	1495	79.7 ± 0.2	−2.2 ± 0.3
363.9	9	13 - 29	−1218	67.9 ± 0.3	−1.9 ± 0.3
395.6	9	13 - 29	−947	57.3 ± 0.3	0.1 ± 0.5
427.2	9	14 - 30	−748	51.7 ± 0.3	−1.6 ± 0.4
454.7	9	15 - 36	−632	46.7 ± 0.1	−1.2 ± 0.1
473.6	9	15 - 47	−582	42.6 ± 0.2	−0.3 ± 0.2
492.1	9	17 - 59	−559	39.9 ± 0.1	−0.1 ± 0.1

a) Estimated density second virial coefficients (see text). b) Calculated using $10^{40} \alpha / C^2 m^2 J^{-1} = 11.62 \pm 0.12$, from reference 12, $10^{40} \alpha^0 / C^2 m^2 J^{-1} = 12.7 \pm 0.6$ (assumed value) and $10^{30} \mu / C m = 4.87 \pm 0.20$, from reference 14.

Table 6.5 Kerr effect of 1,2,4,5-tetrafluorobenzene at 632.8 nm

T / K	Number of Pressures	Pressure Range / kPa	$10^6 B$ [a)] / $m^3\ mol^{-1}$	$10^{27} A_K$ / $C^2\ m^5\ J^{-2}\ mol^{-1}$	$10^{29} B_K$ [b)] / $C^2\ m^8\ J^{-2}\ mol^{-2}$
337.4	10	11 - 27	−1499	19.8 ± 0.2	4 ± 3
355.0	10	11 - 36	−1306	19.0 ± 0.1	−1 ± 1
372.4	10	11 - 48	−1138	18.2 ± 0.1	1 ± 1
381.4	10	19 - 51	−1059	17.9 ± 0.1	−2 ± 1
394.8	7	20 - 40	−953	16.9 ± 0.1	0 ± 1
417.2	9	15 - 49	−803	16.4 ± 0.1	−2 ± 1
445.2	10	15 - 54	−665	15.2 ± 0.1	0 ± 1
472.6	9	16 - 47	−584	14.4 ± 0.2	1 ± 2
491.0	6	27 - 43	−559	13.7 ± 0.1	0 ± 1

a) Estimated density second virial coefficients (see text). b) Calculated using $10^{40}\alpha / C^2\ m^2\ J^{-1} = 11.44 \pm 0.23$, from reference 12, and $10^{40}\alpha^0 / C^2\ m^2\ J^{-1} = 12.5 \pm 0.5$ (assumed value).

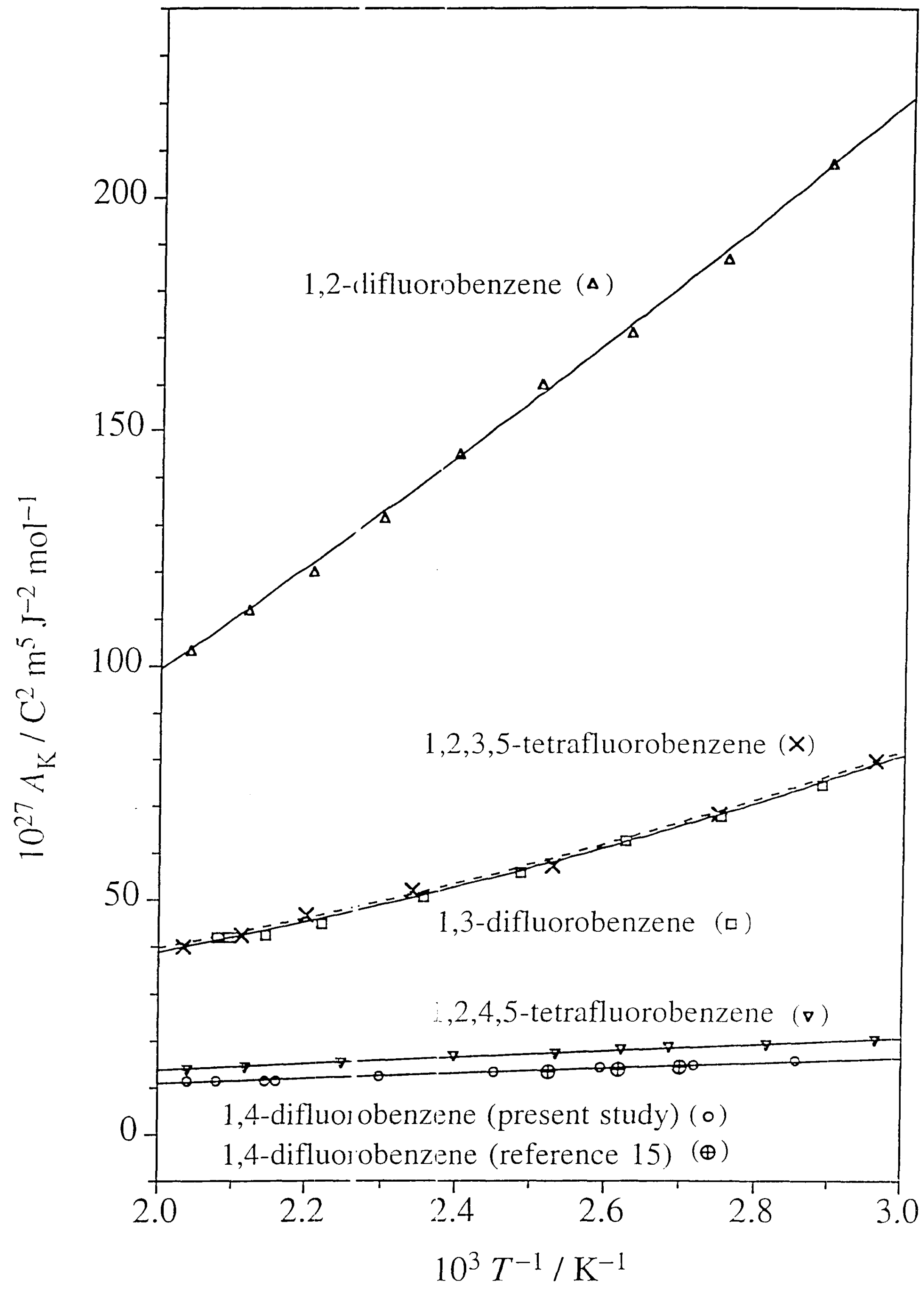

Figure 6 1 The Kerr effects of the fluorobenzenes.

Table 6.6 Rayleigh light-scattering results for 1,2-difluorobenzene and 1,3-difluorobenzene at 632.8 nm, with vibrational Raman lines included. [a)]

	1,2-difluorobenzene	1,3-difluorobenzene
$100\rho_0$	2.12 ± 0.03	2.22 ± 0.03
	2.03 ± 0.02	2.24 ± 0.03
	2.04 ± 0.03	2.24 ± 0.03
	2.13 ± 0.03	
	2.08 ± 0.03	
	2.13 ± 0.04	
	2.10 ± 0.03	
	2.09 ± 0.01	
	2.10 ± 0.02	
average $100\rho_0$	2.09 ± 0.04	2.23 ± 0.02
$\alpha\,/\,10^{-40}\,\mathrm{C^2\,m^2\,J^{-1}}$	11.66 ± 0.50	11.79 ± 0.27
	11.83 ± 0.30	
	11.52 ± 0.12 [b)]	11.37 ± 0.11 [b)]

a) The vibrational Raman lines were not excluded as they are only significant for weakly anisotropic molecules, where $100\rho_0 < 1$. b) From liquid-phase refractive indices, given in reference 12.

difluorobenzene, due to problems caused by pressure fluctuations. The mean polarizabilities of these two difluorobenzenes at 632.8 nm were also measured using the light-scattering apparatus but, as will be explained in the discussion, these values were not used in the analysis of the Kerr-effect results.

6.3 DISCUSSION

For nondipolar molecules with D_{2h} symmetry, the electric properties are related to the Kerr first virial coefficient by

$$ {}_{\mathrm{m}}K = (N_{\mathrm{A}}/81\varepsilon_0)\left\{\gamma^{\mathrm{K}} + (3/10)(kT)^{-1}\left(\alpha_{\alpha\beta}\alpha^0{}_{\alpha\beta} - 3\alpha\alpha^0\right)\right\}. \tag{6.1} $$

The small temperature dependences of the Kerr effects of 1,4-difluorobenzene and 1,2,4,5-tetrafluorobenzene, linear in T^{-1}, contrast with the larger, quadratic dependences of 1,2-difluoro-, 1,3-difluoro- and 1,2,3,5-tetrafluoro-benzene. It is also evident that the temperature dependences of the Kerr effects of 1,3-difluorobenzene and 1,2,3,5-tetrafluorobenzene are almost identical. As even the curvatures shown in Figure 6.1 for these two species are very similar, this suggests that disubstitution of fluorine at the 1,4- positions does not greatly affect the electric properties. It is already known that the mean polarizability and refractivity of the fluorine atom and carbon-fluorine bond are very similar to those of the hydrogen atom and carbon-hydrogen bond, respectively.[16] These two molecules also have similar dipole moments.

The Kerr effects of these fluorobenzenes have not previously been measured in the vapour phase. Aroney et al.[8] have reported the infinite-dilution Kerr constants of 1,2-difluoro-, 1,3-difluoro-, 1,4-difluoro- and 1,2,4,5-tetrafluoro-benzene, at 298 K and 589 nm in cyclohexane. As these values are significantly lower (by ≈ 20 - 40%) than the Kerr first virial coefficients from this study, extrapolated to the same temperature, the Kerr constants of these fluorobenzenes appear to have a significant state dependence.

The results for the dipolar fluorobenzenes were analyzed in the same manner as for dibromomethane, described in Chapter 5. That is, γ^{K} values were interpolated from previous studies on the nondipolar members of the fluorobenzenes series[1] and the Kerr-effect data were fitted to the equation

$$ \begin{aligned} \left[A_{\mathrm{K}} - (N_{\mathrm{A}}/81\varepsilon_0)\gamma^{\mathrm{K}}\right]T = {} & (N_{\mathrm{A}}/81\varepsilon_0 k)\left\{\left[(2/3)\mu\beta^{\mathrm{K}} + (9/5)\alpha\alpha^0\kappa^2\right]\right. \\ & \left. + (3/10k)\mu^2(\alpha_{zz} - \alpha)T^{-1}\right\} \end{aligned} \tag{6.2} $$

to determine α_{zz} and β^{K}. Any errors attributable to these estimated values are likely to be very small, since the bond-additivity approximation is known to be reasonable,[1,17,18] and the effects of such errors are further mitigated by the very small contributions of the

γ^{K} terms to the measured Kerr constants of the fluorobenzenes.[1,2] Figures 6.2, 6.3 and 6.4 depict the analyses of the temperature dependences of the Kerr effects of 1,2-difluoro-, 1,3-difluoro- and 1,2,3,5-tetrafluoro-benzene, respectively. Kerr-effect measurements on 1,2,3,5-tetrafluorobenzene were possible at only seven temperatures, because of the smallness of the sample. However, the gradients of these graphs were all well determined, with small uncertainties. The deviations from the lines of best fit of several points in the graphs are greater than their statistical uncertainties, but the addition of a systematic uncertainty to these values has little effect on the derived quantities.

Although the individual measurements of the depolarization ratio of 1,2-difluorobenzene, shown in Table 6.6, were imprecise, the average ρ_0 value should be reliable. No difficulties were encountered in measuring the depolarization ratio of 1,3-difluorobenzene. The mean polarizabilities of 1,2- and 1,3-difluorobenzene determined by the author using the light-scattering apparatus are in fair, but not good, agreement with those determined from refractive indices at 632.8 nm. Similar discrepancies between mean polarizabilities obtained from the two methods have been reported for other compounds with low volatilities.[19] The mean polarizabilities obtained from the refractive-index measurements were considered more reliable and were used in the analyses of the Kerr-effect results.

Tables 6.7, 6.8 and 6.9 list the electric properties of 1,2-difluoro-, 1,3-difluoro- and 1,2,3,5-tetrafluoro-benzene, respectively. For each of these molecules, the z - axis is coincident with the dipole moment, the x - axis is also in the plane of the benzene ring and the y - axis is orthogonal to the plane of the benzene ring. Gentle et al.[2] reported that α_{zz} was slightly larger than α_{xx} in fluorobenzene. A similar enhancement of the α_{zz} component with respect to the α_{xx} component in 1,2-difluorobenzene is therefore expected, and is indeed observed. This is also in agreement with the solution-phase work of Aroney et al.,[8] who obtained $\alpha = 10.90$, $\alpha_{xx} = 12.34$, $\alpha_{yy} = 7.61$ and $\alpha_{zz} = 12.76 \times 10^{-40}\,\mathrm{C^2\,m^2\,J^{-1}}$. The polarizabilities determined in the present work are much more reliable, as the solution-phase values are influenced by local-field effects and the hyperpolarizabilities were not taken into account in their evaluation.

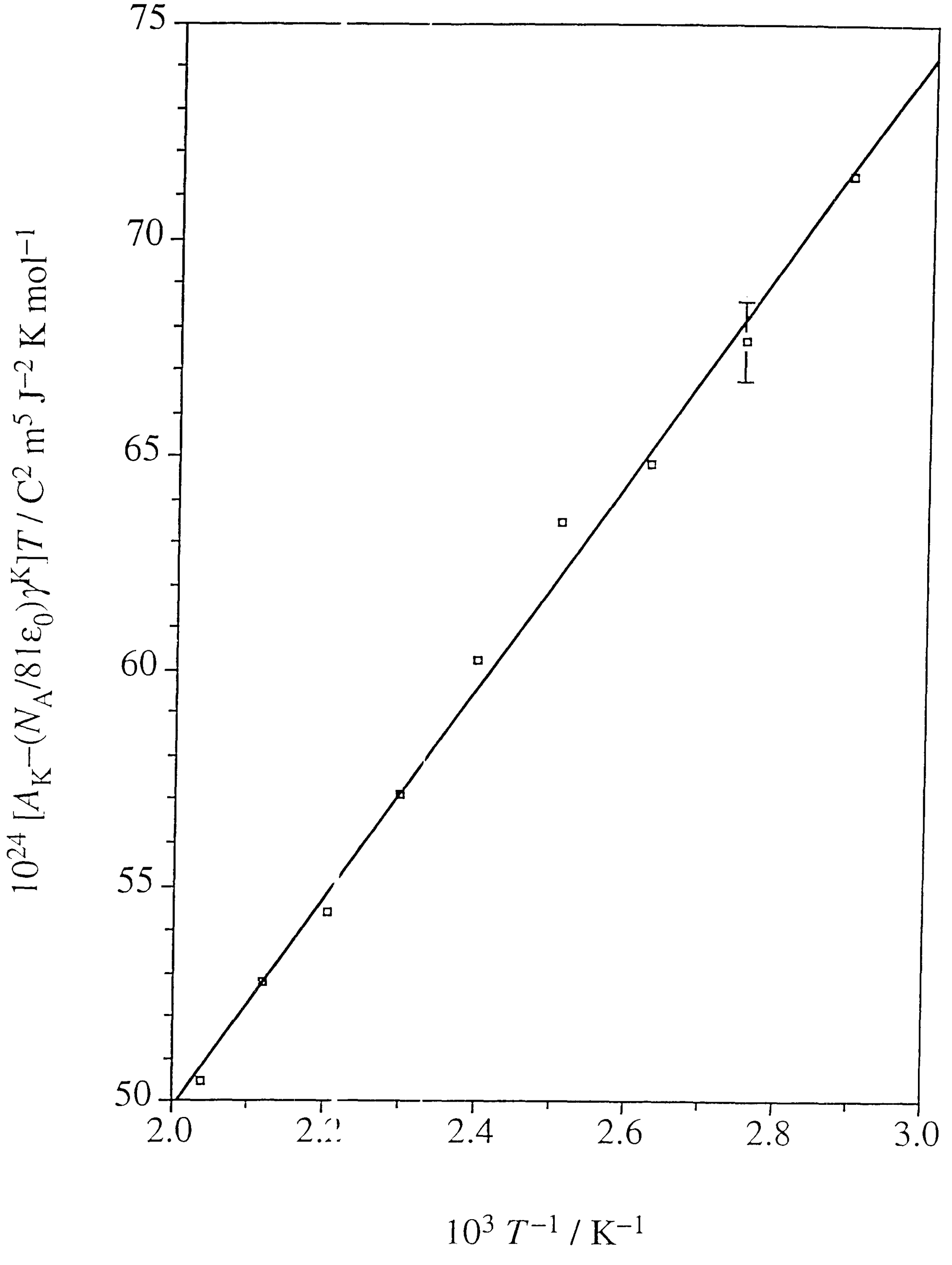

Figure 6.2 Analysis of the Kerr effect of 1,2-difluorobenzene.

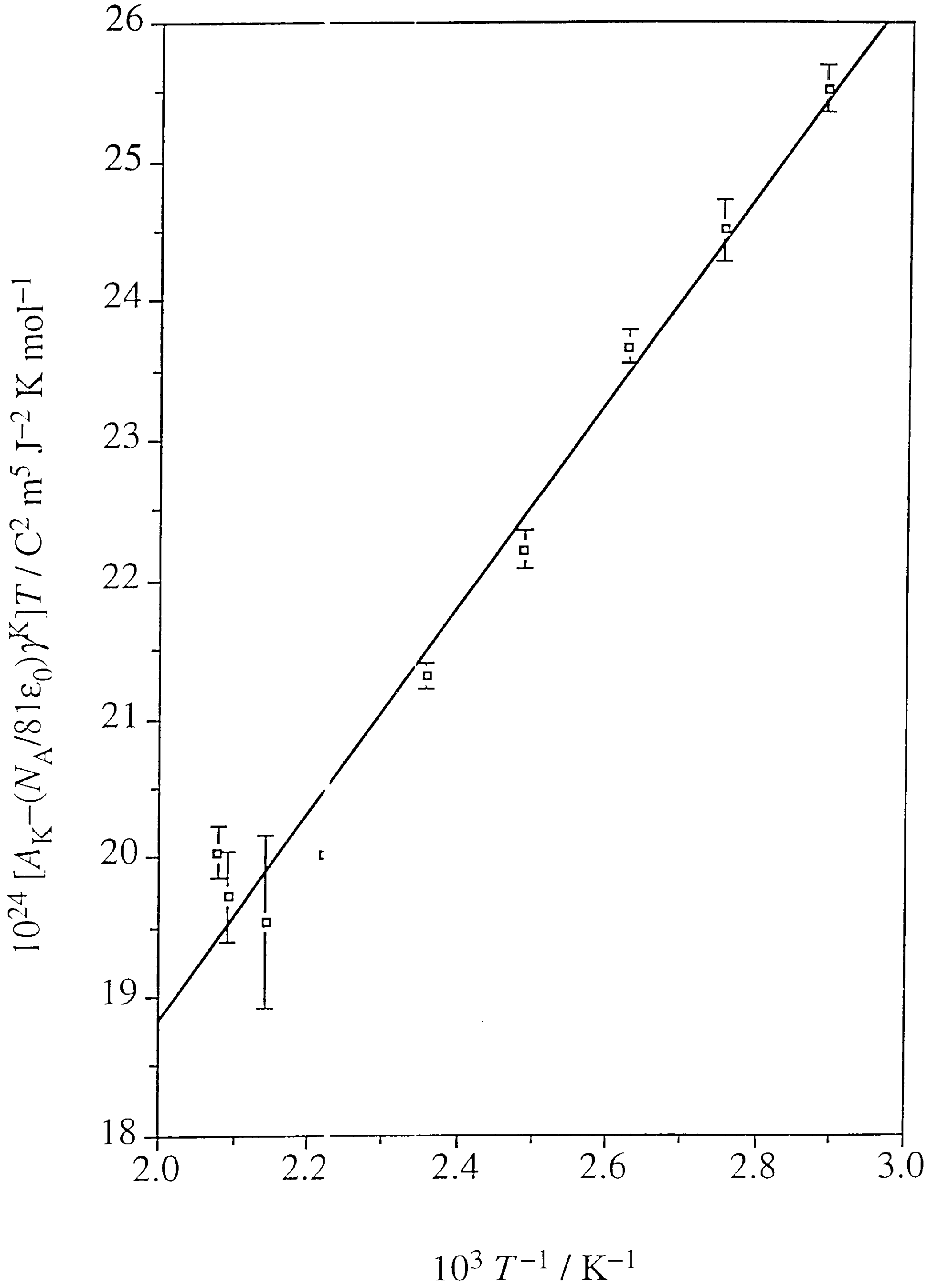

Figure 6.3 Analysis of the Kerr effect of 1,3-difluorobenzene.

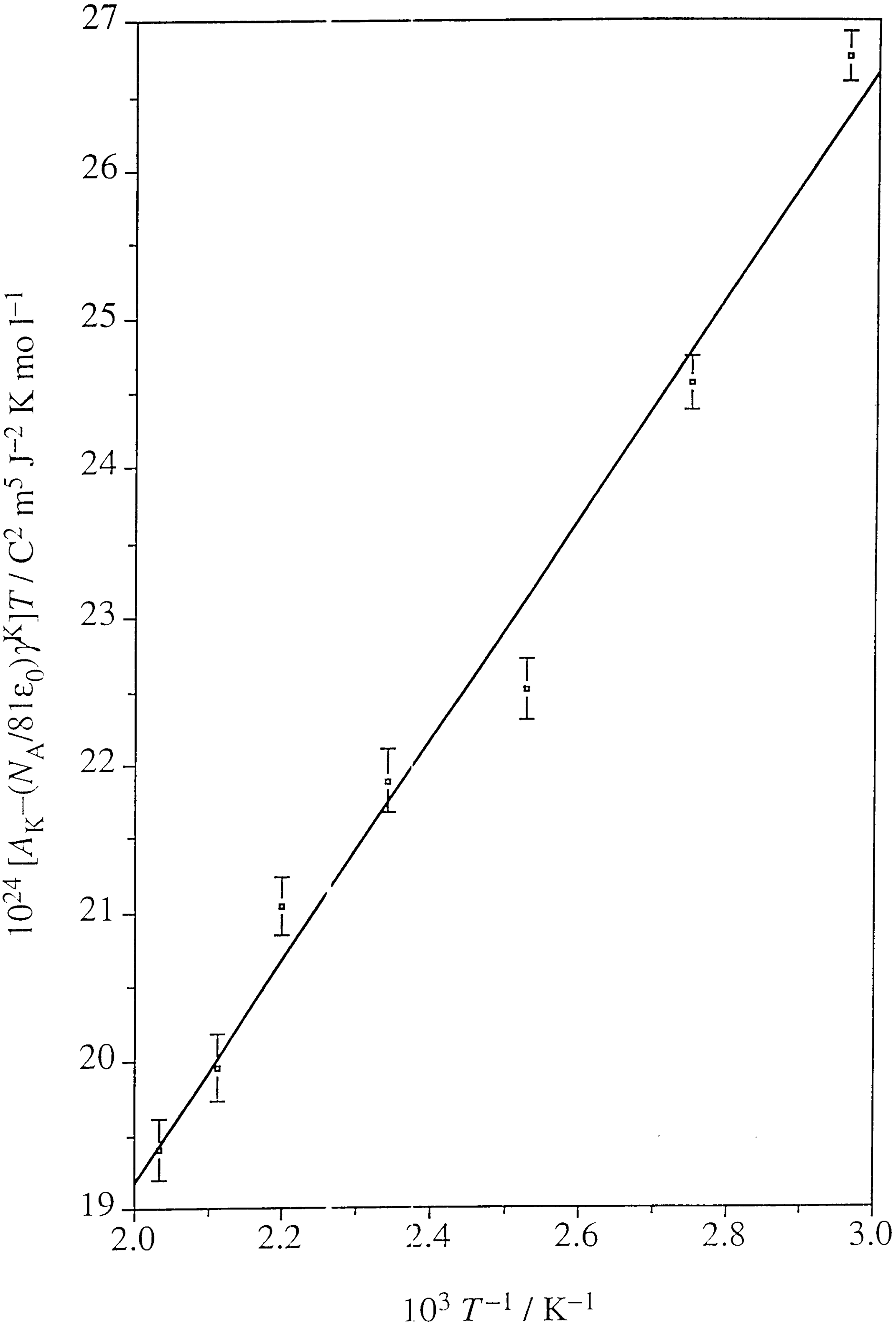

Figure 6.4 Analysis of the Kerr effect of 1,2,3,5-tetrafluorobenzene.

Table 6.7 Analysis of the Kerr effect of 1,2-difluorobenzene at 632.8 nm

Property	Value
10^{21} slope / $C^2\ m^5\ J^{-2}\ K^{-1}\ mol^{-1}$ a)	24.5 ± 0.7
10^{24} intercept / $C^2\ m^5\ J^{-2}\ K^{-2}\ mol^{-1}$ a)	0.9 ± 1.7
$10^{40}\ \alpha$ / $C^2\ m^2\ J^{-1}$ b)	11.52 ± 0.12
$10^{40}\ \alpha^0$ / $C^2\ m^2\ J^{-1}$ c)	12.6 ± 0.6
$10^2\ \kappa^2$	3.58 ± 0.07
$10^{30}\ \mu$ / C m d)	8.64 ± 0.07
$10^{60}\ \gamma^K$ / $C^4\ m^4\ J^{-3}$ c)	0.5
$10^{40}\ (\alpha_{zz} - \alpha)$ / $C^2\ m^2\ J^{-1}$	2.48 ± 0.07
$10^{40}\ \alpha_{xx}$ / $C^2\ m^2\ J^{-1}$	13.38 ± 0.33
$10^{40}\ \alpha_{yy}$ / $C^2\ m^2\ J^{-1}$	7.17 ± 0.07
$10^{40}\ \alpha_{zz}$ / $C^2\ m^2\ J^{-1}$	14.00 ± 0.14
$10^{50}\ \beta^K$ / $C^3\ m^3\ J^{-2}$	-1.4 ± 0.5

a) From equation 6.2. b) Reference 12. c) Estimated value (see text). d) Reference 13.

Table 6.8 Analysis of the Kerr effect of 1,3-difluorobenzene at 632.8 nm

Property	Value
10^{21} slope / $C^2\ m^5\ J^{-2}\ K^{-1}\ mol^{-1}$ a)	7.88 ± 0.41
10^{24} intercept / $C^2\ m^5\ J^{-2}\ K^{-2}\ mol^{-1}$ a)	2.8 ± 1.0
$10^{40}\ \alpha$ / $C^2\ m^2\ J^{-1}$ b)	11.37 ± 0.11
$10^{40}\ \alpha^0$ / $C^2\ m^2\ J^{-1}$ c)	12.4 ± 0.6
$10^2\ \kappa^2$	3.83 ± 0.03
$10^{30}\ \mu$ / C m d)	5.04 ± 0.07
$10^{60}\ \gamma^K$ / $C^4\ m^4\ J^{-3}$ c)	0.5
$10^{40}\ (\alpha_{zz} - \alpha)$ / $C^2\ m^2\ J^{-1}$	2.35 ± 0.12
$10^{40}\ \alpha_{xx}$ / $C^2\ m^2\ J^{-1}$	13.47 ± 0.33
$10^{40}\ \alpha_{yy}$ / $C^2\ m^2\ J^{-1}$	6.92 ± 0.07
$10^{40}\ \alpha_{zz}$ / $C^2\ m^2\ J^{-1}$	13.72 ± 0.18
$10^{50}\ \beta^K$ / $C^3\ m^3\ J^{-2}$	-1.5 ± 0.5

a) From equation 6.2. b) Reference 12. c) Estimated value (see text). d) Reference 13.

Table 6.9 Analysis of the Kerr effect of 1,2,3,5-tetrafluorobenzene at 632.8 nm

Property	Value
10^{21} slope / C^2 m^5 J^{-2} K^{-1} mol^{-1} a)	7.58 ± 0.43
10^{24} intercept / C^2 m^5 J^{-2} K^{-2} mol^{-1} a)	4.0 ± 1.1
10^{40} α / C^2 m^2 J^{-1} b)	11.62 ± 0.12
10^{40} α^0 / C^2 m^2 J^{-1} c)	12.7 ± 0.6
10^2 κ^2 d)	3.74 ± 0.04
10^{30} μ / C m e)	4.87 ± 0.20
10^{60} γ^K / C^4 m^4 J^{-3} c)	0.5
10^{40} $(\alpha_{zz} - \alpha)$ / C^2 m^2 J^{-1}	2.42 ± 0.14
10^{40} α_{xx} / C^2 m^2 J^{-1}	13.69 ± 0.40
10^{40} α_{yy} / C^2 m^2 J^{-1}	7.13 ± 0.07
10^{40} α_{zz} / C^2 m^2 J^{-1}	14.04 ± 0.27
10^{50} β^K / C^3 m^3 J^{-2}	-1.0 ± 0.6

a) From equation 6.2. b) Reference 12. c) Estimated value (see text). d) Reference 19.

e) Reference 14.

The same argument can also be used to predict $\alpha_{zz} < \alpha_{xx}$ for 1,3-difluorobenzene. This is not observed, although the enhancement of α_{zz} in 1,3-difluorobenzene is less than that for 1,2-difluorobenzene and the statistical uncertainties provide a large degree of overlap between the numerical values of α_{xx} and α_{zz}. These are the first reported polarizabilities for 1,3-difluorobenzene. The in-plane polarizabilities of 1,2,3,5-tetrafluorobenzene are also very similar. However, as the results of Gentle et al.[2] for fluorobenzene and pentafluorobenzene predict, α_{zz} is larger than α_{xx} for 1,2,3,5-tetrafluorobenzene.

The Kerr first hyperpolarizabilities of 1,2-difluoro-, 1,3-difluoro- and 1,2,3,5-tetrafluoro-benzene are all of the same sign and are in good agreement with those of fluorobenzene and pentafluorobenzene,[2] $\beta^{\mathrm{K}} = (-0.9 \pm 0.4)$ and $(-0.8 \pm 0.4) \times 10^{-50}$ $\mathrm{C^3\,m^3\,J^{-2}}$, respectively. As Gentle noted,[11] these values are larger than the Kerr first hyperpolarizabilities typically found for aliphatic molecules. The large uncertainties associated with the β^{K} values are due to the unavoidable imprecision of the intercepts in Figures 6.2, 6.3 and 6.4 and the relatively small contributions that the $\mu\beta^{\mathrm{K}}$ term makes to the measured Kerr constants of these molecules, as will be shown later.

Gentle et al.[2] have previously discussed the regular variation of the polarizability components with progressive fluorine substitution in the fluorobenzenes series. The free-molecule polarizabilities that have been measured for the fluorobenzenes (benzene,[1] fluoro-,[2] 1,2-difluoro-, 1,3-difluoro-, 1,3,5-trifluoro-,[1] 1,2,3,5-tetrafluoro-, pentafluoro-[2] and hexafluoro-benzene[1]) are shown in Figure 6.5. The values of the α_{zz} component are represented by the circles and unbroken line and those of α_{xx} by the triangles and the dashed line. It is obvious that the polarizabilities reported in this work are in excellent agreement with those of the other fluorobenzenes, and several trends are apparent. Progressive introduction of fluorine atoms into the benzene ring has only a small effect on the mean polarizability, and results in a small enhancement of the two in-plane components. Progressive fluorine substitution appears to give a slight increase in the α_{xx} component with respect to the α_{zz} component, and to decrease the out-of-plane α_{yy} component, presumably due to conjugative and inductive interactions.[2]

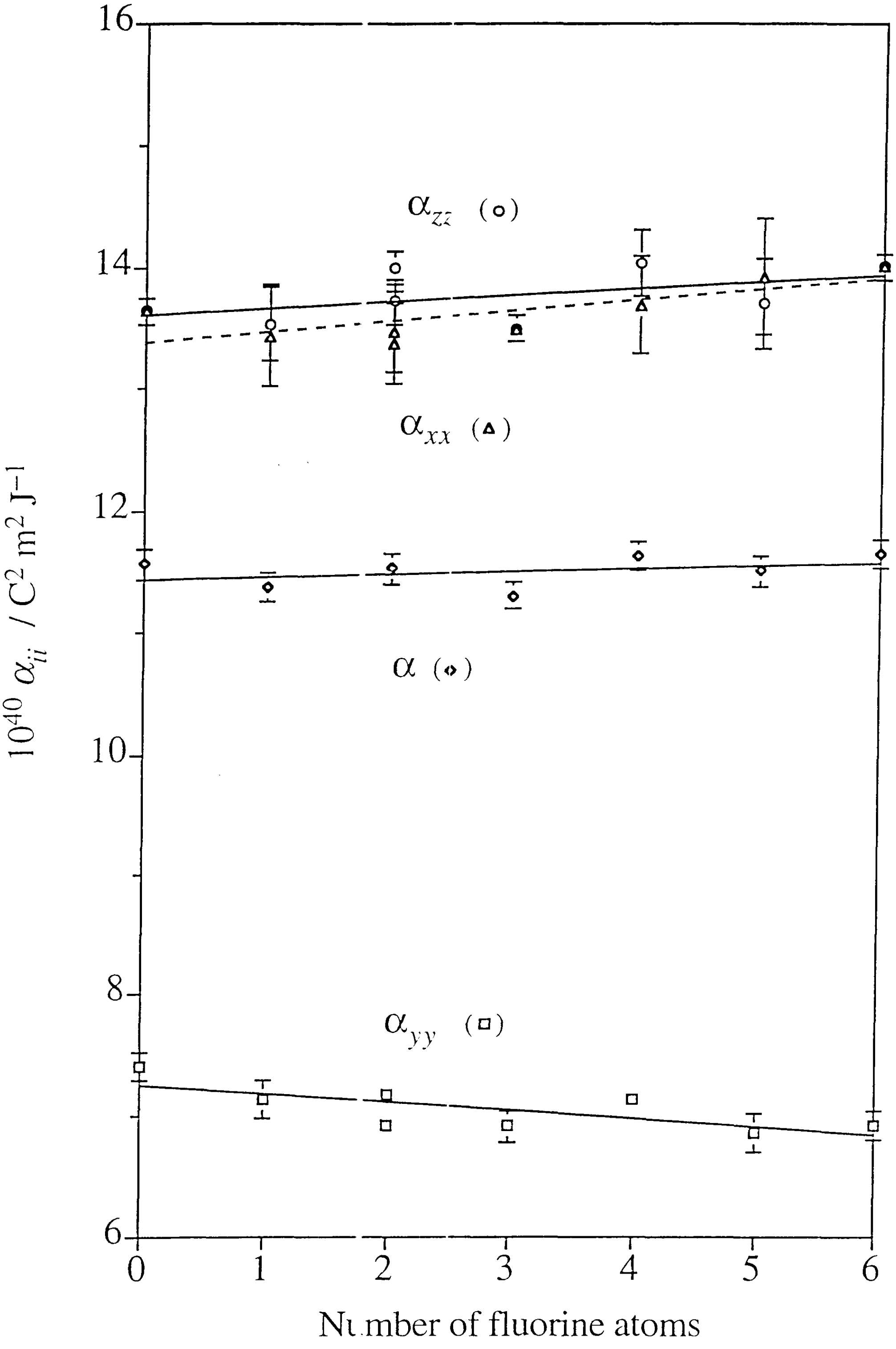

Figure 6.5 Variation of the polarizabilities of the fluorobenzenes with fluorine substitution.

For nondipolar molecules with D_{2h} symmetry, the Kerr first virial coefficient is related to the electric properties by equation 6.1. However, the static polarizability components of 1,4-difluorobenzene and 1,2,4,5-tetrafluorobenzene are unknown, and the assumption that $\alpha_{\alpha\beta} = \alpha^0_{\alpha\beta}$ results in unrealistic optical-frequency polarizabilities for these molecules. This suggests that dispersion and vibrational contributions have a greater effect on the polarizability components of the fluorobenzenes than fluorine substitution. In view of the similarities of the in-plane polarizabilities of the other fluorobenzene molecules, it was assumed that $\alpha_{xx} = \alpha_{zz}$ for these two species. The temperature dependences of the Kerr effects of 1,4-difluorobenzene and 1,2,4,5-tetrafluorobenzene are, therefore, related to the product of the static and optical-frequency polarizability anisotropies by

$$A_K = \left(N_A/405\varepsilon_0\right)\left\{5\gamma^K + (kT)^{-1}\left(\Delta\alpha\Delta\alpha^0\right)\right\}. \tag{6.3}$$

These terms were separated using the Rayleigh light-scattering measurements of Keir.[19]

The ratios, $\Delta\alpha^0/\Delta\alpha$, of the static to the optical-frequency polarizability anisotropies for these molecules are listed in Tables 6.10 and 6.11. Gentle et al.[1] found that the ratios for benzene and 1,3,5-trifluorobenzene are 0.88 ± 0.05 and 1.16 ± 0.05, respectively. The ratio for 1,4-difluorobenzene is half-way between these two values, at 0.99 ± 0.05. Good agreement is observed between the ratio of 1.22 ± 0.03 for 1,2,4,5-tetrafluorobenzene and those of 1,3,5-trifluorobenzene, 1.16 ± 0.05, and hexafluorobenzene, 1.18 ± 0.06. Gentle[1] analyzed the electronic and vibrational contributions to $\Delta\alpha^0$ for benzene and hexafluorobenzene. A similar analysis for the fluorobenzenes measured in this work was not attempted, due to an absence of data on the electronic and infrared transitions of these species.

Despite the long extrapolation involved in the analysis, the Kerr second hyperpolarizability of 1,4-difluorobenzene, $(0.6 \pm 0.7) \times 10^{-60}\,\mathrm{C^4\,m^4\,J^{-3}}$, is in excellent agreement with those of benzene, (0.4 ± 0.4); 1,3,5-trifluorobenzene, (0.5 ± 0.2); and hexafluorobenzene, $(0.7 \pm 0.7) \times 10^{-60}\,\mathrm{C^4\,m^4\,J^{-3}}$.[1] The Kerr second

Table 6.10 Analysis of the Kerr effect of 1,4-difluorobenzene at 632.8 nm

Property	Value
10^{24} slope / $C^2\ m^5\ J^{-2}\ K^{-1}\ mol^{-1}$ a)	5.14 ± 0.24
10^{27} intercept / $C^2\ m^5\ J^{-2}\ mol^{-1}$ a)	0.51 ± 0.59
$10^{40}\ \alpha$ / $C^2\ m^2\ J^{-1}$ b)	11.34 ± 0.12
$10^2\ \kappa^2$ c)	3.64 ± 0.03
$10^{60}\ \gamma^K$ / $C^4\ m^4\ J^{-3}$	0.6 ± 0.7
$10^{80}\ \Delta\alpha\Delta\alpha^0$ / $C^4\ m^4\ J^{-2}$ a)	43.8 ± 2.0
$10^{40}\ \Delta\alpha$ / $C^2\ m^2\ J^{-1}$ c)	-6.52 ± 0.10
$10^{40}\ \Delta\alpha^0$ / $C^2\ m^2\ J^{-1}$	-6.48 ± 0.31
$\Delta\alpha^0/\Delta\alpha$	0.99 ± 0.05

a) From equation 6.3. b) Reference 12. c) Reference 20.

Table 6.11 Analysis of the Kerr effect of 1,2,4,5-tetrafluorobenzene at 632.8 nm

Property	Value
10^{24} slope / C^2 m^5 J^{-2} K^{-1} mol^{-1} a)	6.84 ± 0.15
10^{27} intercept / C^2 m^5 J^{-2} mol^{-1} a)	-0.18 ± 0.34
10^{40} α / C^2 m^2 J^{-1} b)	11.44 ± 0.23
10^2 κ^2 c)	3.72 ± 0.08
10^{60} γ^K / C^4 m^4 J^{-3}	-0.2 ± 0.4
10^{80} $\Delta\alpha\Delta\alpha^0$ / C^4 m^4 J^{-2} a)	56.2 ± 1.2
10^{40} $\Delta\alpha$ / C^2 m^2 J^{-1} c)	-6.788 ± 0.023
10^{40} $\Delta\alpha^0$ / C^2 m^2 J^{-1}	-8.28 ± 0.18
$\Delta\alpha^0/\Delta\alpha$	1.22 ± 0.03

a) From equation 6.3. b) Reference 12. c) Reference 19.

hyperpolarizability of 1,2,4,5-tetrafluorobenzene, $(-0.2 \pm 0.4) \times 10^{-60}\,\mathrm{C}^4\,\mathrm{m}^4\,\mathrm{J}^{-3}$, is also in good agreement, when the uncertainties are taken into account. It has already been established[16] that the polarizability of the fluorine atom is very similar to that of the hydrogen atom, and these results demonstrate that the Kerr second hyperpolarizabilities of the fluorobenzenes show a very small variation with the number of fluorine atoms. As noted in Chapter 5, Buckingham and Orr[17] have also found the Kerr second hyperpolarizabilities of methane and tetrafluoromethane to be very similar.

The γ^{K} term makes a very small contribution to the Kerr first virial coefficients of the fluorobenzenes at 300 K, as shown in Table 6.12. This was also found to be the case for the fluorobenzenes investigated by Gentle et al.,[1,2] which are also presented in this table. For the dipolar fluorobenzenes, the $\mu\beta^{\mathrm{K}}$ term is an order of magnitude larger than the γ^{K} term, yet it is still smaller than the $\alpha\alpha^0\kappa^2$ and dominant $\mu^2(\alpha_{zz} - \alpha)$ terms. Table 6.12 also shows that the various contributions to the Kerr first virial coefficients of 1,3-difluorobenzene and 1,2,3,5-tetrafluorobenzene are very similar. This results in the temperature dependences of the Kerr effects of these two species being almost identical, as shown in Figure 6.1. These results confirm that disubstitution of fluorine atoms into the 1,4-positions of benzene has only a very small effect on these contributions. For the nondipolar fluorobenzenes with D_{2h} symmetry, 1,4-difluoro- and 1,2,4,5-tetrafluoro-benzene, the dominant contribution to A_{K} is from the $(9N_{\mathrm{A}}/405\varepsilon_0 kT)\alpha\alpha^0\kappa^2$ term. This is equivalent to the $(N_{\mathrm{A}}/405\varepsilon_0 kT)\Delta\alpha\Delta\alpha^0$ contribution for nondipolar species with C_{3v} or higher symmetry, which was used in the analysis of the Kerr effects of 1,4-difluoro- and 1,2,4,5-tetrafluoro-benzene.

Due to the limited density dependences that were possible in these studies, the Kerr second virial coefficients of the fluorobenzenes investigated in this work are uncertain and unreliable. Gentle[11] was also unable to obtain accurate B_{K} values for the other fluorobenzenes. Little can be concluded from these B_{K} values, other than that they tend to be large and negative for 1,2-difluoro-, 1,4-difluoro- and 1,2,3,5-tetrafluoro-benzene and unreliable for 1,3-difluoro- and 1,2,4,5-tetrafluoro-benzene. The results for 1,2- and 1,4-difluorobenzene, in particular, suggest that B_{K} for these

Table 6.12 Contributions of individual terms to A_K for benzene and the fluorobenzenes at 300 K [a)]

Term	B [b)]	FB [c)]	1,2-DFB	1,3-DFB	1,4-DFB	1,3,5-TFB [b)]	1,2,3,5-TFB	1,2,4,5-TFB	PFB [c)]	HFB [b)]
$(N_A/81\varepsilon_0)\gamma^K$	0.3 2%	0.3 0.3%	0.4 0.2%	0.4 0.4%	0.5 3%	0.4 2%	0.4 0.4%	−0.2 −1%	0.5 1%	0.6 2%
$(2N_A/243\varepsilon_0 kT)\mu\beta^K$	–	−6.3 −6%	−15.9 −6%	−10.5 −11%	–	–	−6.8 −7%	–	−5.5 −6%	–
$(9N_A/405\varepsilon_0 kT)\alpha\alpha^0\kappa^2$	13.9 98%	18.0 18%	19.0 7%	19.8 20%	17.1 97%	19.9 98%	20.1 21%	22.8 101%	21.4 24%	23.9 98%
$\left(N_A/270\varepsilon_0 k^2T^2\right)\mu^2(\alpha_{zz}-\alpha)$	–	88.5 88%	272.2 99%	87.6 90%	–	–	84.2 86%	–	74.5 82%	–
A_K	14.1	100.5	275.8	97.3	17.6	20.3	98.0	22.6	90.9	24.5

B = benzene; FB = fluorobenzene; 1,2-DFB = 1,2-difluorobenzene; 1,3-DFB = 1,3-difluorobenzene; 1,4-DFB = 1,4-difluorobenzene; 1,3,5-TFB = 1,3,5-trifluorobenzene; 1,2,3,5-TFB = 1,2,3,5-tetrafluorobenzene; 1,2,4,5-TFB = 1,2,4,5-tetrafluorobenzene; PFB = pentafluorobenzene and HFB = hexafluorobenzene.

a) Expressed in units of 10^{-27} C^2 m^5 J^{-2} mol^{-1}. b) Reference 1. c) Reference 2.

molecules may become more positive as the temperature increases, although more accurate and more extensive density dependences are required to confirm this trend.

6.4 CONCLUSIONS

This work, an extension of earlier studies,[1,2] has resulted in the most comprehensive experimental investigation yet reported of the influence of functional-group substitution on the anisotropic electric polarizabilities and the hyperpolarizabilities of free molecules. The free-molecule polarizabilities of 1,2-difluoro-, 1,3-difluoro- and 1,2,3,5-tetrafluoro-benzene were measured for the first time. Comparison of these results with those of other molecules in the series shows that fluorine substitution has only a very small effect on each of the components of the polarizability. Fluorine substitution appears to have a greater influence on the static polarizability anisotropy, however. Despite the small contributions of the γ^{K} and $\mu\beta^{K}$ terms to the Kerr first virial coefficients of these molecules, the hyperpolarizabilities were also found to be in good agreement with those of the other fluorobenzenes. As the earlier study indicated,[2] the Kerr first hyperpolarizabilities of these aromatic molecules are larger than those typically found for aliphatic molecules.

6.5 REFERENCES

1 Gentle, I.R. and Ritchie, G.L.D., *J. Phys. Chem.*, **93**, 7740 (1989).

2 Gentle, I.R., Hesling, M.R. and Ritchie, G.L.D., *J. Phys. Chem.*, **94**, 1844 (1990).

3 Bogaard, M.P., Buckingham, A.D., Corfield, M.G., Dunmur, D.A. and White, A.H., *Chem. Phys. Lett.*, **12**, 558 (1972).

4 Lukins, P.B., Buckingham, A.D. and Ritchie, G.L.D., *J. Phys. Chem.*, **88**, 2414 (1984).

5 Lukins, P.B. and Ritchie, G.L.D., *J. Phys. Chem.*, **89**, 1312 (1985).

6 Battaglia, M.R., Buckingham, A.D. and Williams, J.H., *Chem. Phys. Lett.*, **78**, 421 (1981).

7 Watson, J.N., *Ph.D. Thesis* (University of New England, 1995).

8 Aroney, M.J., Cleaver, G., Pierens, R.K. and Le Fèvre, R.J.W., *J. Chem. Soc., Perkin Trans. II*, 3 (1974).

9 Dymond, J.H. and Smith, E.B., *The Virial Coefficients of Pure Gases and Mixtures* (Clarendon Press, Oxford, 1980).

10 Hirschfelder, J.O., Curtiss, C.F. and Bird, R.B., *Molecular Theory of Gases and Liquids* (Wiley, New York, 1964).

11 Gentle, I.R., *Ph.D. Thesis* (University of Sydney, 1987).

12 Landolt-Börnstein, *Zahlenwerte und Funktionen*, Band II, Teil 8 (Springer, Berlin, 1962).

13 Nygaard, L., Hansen, E.R., Hansen, R.L., Rastrup-Andersen, J. and Sørensen, G.O., *Spectrochim. Acta*, **23**, 2813 (1967).

14 Sharma, S.D. and Doraiswamy, S., *Can. J. Phys.*, **55**, 1211 (1977).

15 Gentle, I.R. and Ritchie, G.L.D., unpublished results.

16 Le Fèvre, R.J.W., *Molecular Refractivity and Polarizability* in *Advances in Physical Organic Chemistry* (V. Gold editor), (Academic Press, London, 1965).

17 Buckingham, A.D. and Orr, B.J., *Trans. Faraday Soc.*, **65**, 673 (1969).

18 Bogaard, M.P., Orr, B.J., Buckingham, A.D. and Ritchie, G.L.D., *J. Chem. Soc., Faraday Trans. 2*, **74**, 1573 (1978).

19 Keir, R.I., *Ph.D. Thesis* (University of New England, 1995).

20 Hesling, M.H., *Ph.D. Thesis* (University of New England, 1990).

CHAPTER 7 - POLARIZABILITY AND HYPERPOLARIZABILITY OF PYRIDINE

7.1 INTRODUCTION

The electric and magnetic properties of the cyclic azines are of great interest.[1-7] The polarizabilities of pyridine, in particular, have attracted considerable attention and discussion. In 1933, Stuart and Volkmann[8] reported a set of polarizability components from a vapour-phase Kerr-effect measurement at a single temperature. Le Fèvre and Le Fèvre[9] subsequently determined values that were in surprisingly good agreement with these, from the Kerr constant of pyridine at infinite dilution in carbon tetrachloride. Battaglia and Ritchie[10] similarly measured the solution-phase Kerr and Cotton-Mouton constants of pyridine in carbon tetrachloride, cyclohexane and dioxane. The results of Stuart and Volkmann were also reanalyzed by Burnham and Gierke,[11] to obtain yet a different set of polarizabilities. More recently, there have been several ab initio calculations of the static and optical-frequency polarizabilities of pyridine.[4,5,12] In the latest experimental study, Coonan[13] has combined measurements of the temperature dependence of the Cotton-Mouton effect of pyridine with the molecular magnetizabilities, previously derived from a microwave Zeeman-effect study.[14] However, the various limitations in the methods of analysis used in several of these earlier studies have yielded inconclusive results. Therefore, it is of interest to investigate the temperature dependence of the vapour-phase Kerr effect of pyridine in order accurately to derive the free-molecule polarizabilities of this species.

Little is known about the Kerr hyperpolarizabilities of pyridine from these earlier studies. A theoretical value for the Kerr second hyperpolarizability has only recently been reported,[7] and electric field-induced second harmonic generation has also been used to measure the hyperpolarizabilities of pyridine.[15] It was, therefore, a secondary aim of this study to measure the Kerr first hyperpolarizability of pyridine. As explained later, γ^K for this species is expected to be negligibly small.

7.2 EXPERIMENTAL

The sample of pyridine was dried over solid potassium hydroxide for 8 days, refluxed over solid potassium hydroxide for 1 hr and then distilled twice over solid potassium hydroxide and Linde Type 4A molecular sieves. The sample was stored under high-purity nitrogen in the dark, and passed through a sintered-glass filter before use. Gas chromatography showed the purity to be > 99.95%.

Density second virial coefficients for pyridine are available for the temperature range 349.1 - 437.8 K.[16] At higher temperatures, the Stockmayer potential[17] was used to calculate the virial coefficients. As the maximum vapour pressure used was only 36 kPa, any errors in these estimated values would have a negligible effect upon the gas densities. The results are listed in Table 7.1, and the temperature dependence of the Kerr effect of pyridine is shown in Figure 7.1.

The mean polarizability of pyridine at 632.8 nm was interpolated from refractivity data,[18] and the dipole moment was obtained from measurements of the vapour-phase dielectric polarization.[19] In addition, the authors of the latter paper reported a value of the mean static polarizability of pyridine, and this was assigned an uncertainty of ± 5%.

The Kerr second virial coefficients of pyridine are poorly defined and unreliable, due to the small ranges of pressure used. No obvious trend is evident in these values and the sign of B_K for pyridine cannot be conclusively determined, at least for the temperature range that was investigated. This imprecision in the values of B_K for pyridine reduces the reliability of those of A_K, although the effects of this on the derived quantities are small, again due to the limited pressure ranges used.

7.3 DISCUSSION

Stuart and Volkmann[8] reported the Kerr constant of pyridine as ${}_{m}K = 71.0 \times 10^{-27}\ C^2\ m^5\ J^{-2}\ mol^{-1}$, using white light, at 419 K. This is in good

Table 7.1 Kerr effect of pyridine at 632.8 nm

T / K	Number of Pressures	Pressure Range / kPa	$10^6 B$ [a] / $m^3\ mol^{-1}$	$10^{27} A_K$ / $C^2\ m^5\ J^{-2}\ mol^{-1}$	$10^{28} B_K$ [b] / $C^2\ m^8\ J^{-2}\ mol^{-2}$
406.9	10	13 - 32	−843	77.9 ± 0.2	−2.2 ± 0.3
413.4	9	14 - 30	−804	73.1 ± 0.3	0.3 ± 0.4
431.4	9	14 - 31	−701	68.0 ± 0.2	0.5 ± 0.3
449.5	10	14 - 30	−608	62.7 ± 0.3	0.3 ± 0.4
461.7	9	14 - 36	−568	59.4 ± 0.2	−0.5 ± 0.3
470.4	7	18 - 34	−540	59.2 ± 0.2	−0.9 ± 0.3
479.8	9	14 - 32	−513	56.4 ± 0.1	−0.5 ± 0.2
489.3	8	15 - 31	−489	53.3 ± 0.3	−0.7 ± 0.4

a) Density second virial coefficients from reference 16 and calculated values (see text). b) Calculated using $10^{40}\alpha$ / $C^2\ m^2\ J^{-1} = 10.55 \pm 0.11$, from reference 18, $10^{40}\alpha^0$ / $C^2\ m^2\ J^{-1} = 12.0 \pm 0.6$ and $10^{30}\mu$ / C m = 7.44 ± 0.07, from reference 19.

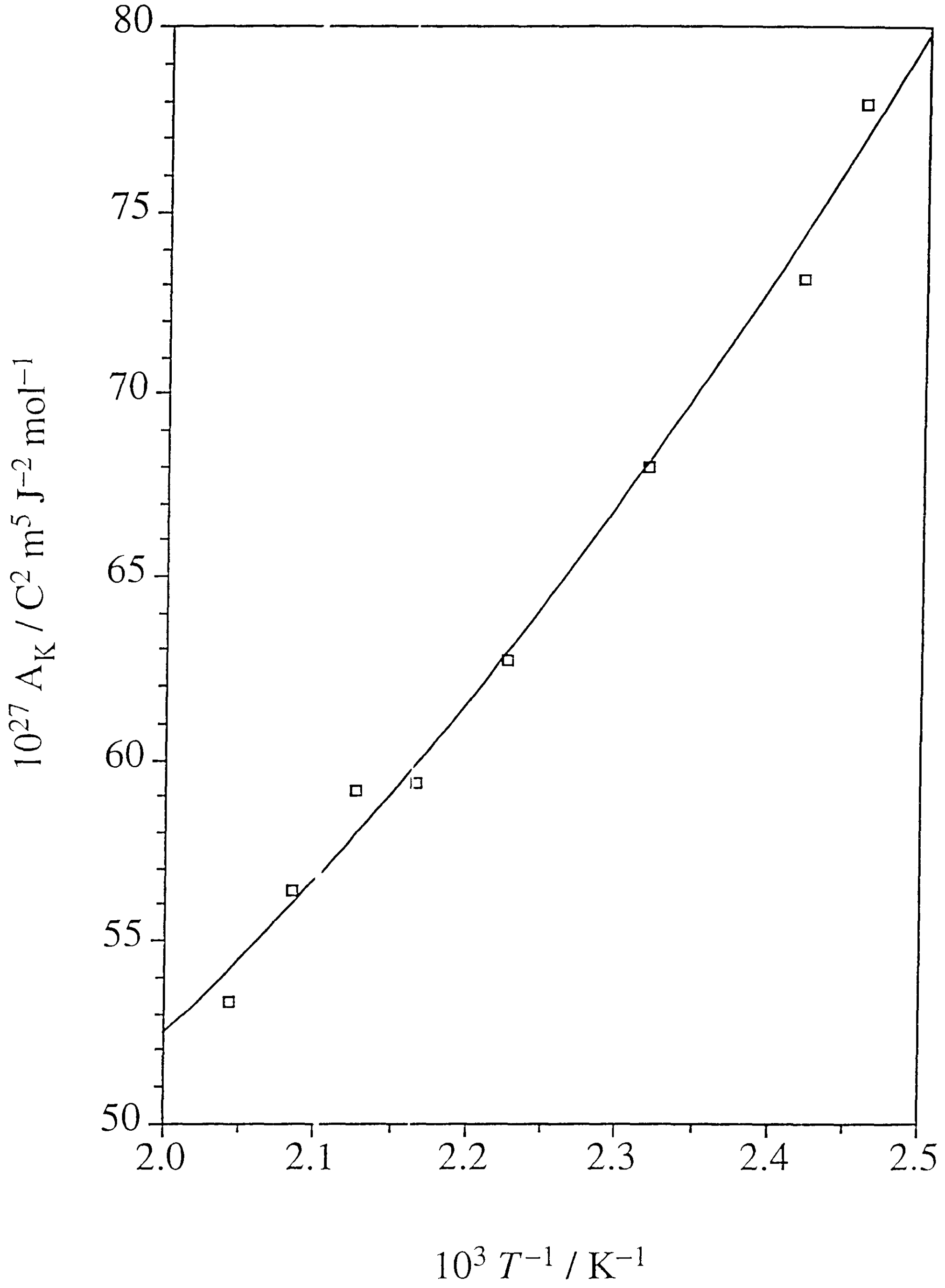

Figure 7.1 Temperature dependence of the Kerr effect of pyridine.

agreement with the value of $A_K = 72.1 \times 10^{-27}\ \mathrm{C^2\,m^5\,J^{-2}\,mol^{-1}}$, at 632.8 nm and the same temperature, interpolated from this work.

The Kerr effect of pyridine was analyzed in the same manner as those of dibromomethane and the dipolar fluorobenzenes, described in Chapters 5 and 6, respectively. As discussed in these earlier chapters, this requires a value for the Kerr second hyperpolarizability. The bond additivity approximation has been shown in this thesis to provide reliable estimates of Kerr second hyperpolarizabilities. Gentle et al.[20] measured $\gamma^K \approx 0$ for benzene, and Halliburton[21] measured $\gamma^K \approx 0$ for s-triazine, at 632.8 nm from vapour-phase Kerr-effect measurements. Therefore, the assumption that $\gamma^K \approx 0$ for pyridine at the same wavelength should be reasonable. The effect of any error in this value is mitigated by the very small contribution that the γ^K term typically makes to the Kerr constants of aromatic molecules, as shown in Chapter 6. Keshari et al.[7] have calculated $\gamma^K = 0.14 \times 10^{-60}\ \mathrm{C^4\,m^4\,J^{-3}}$ for pyridine at a wavelength of 602 nm, which makes only a 0.2% contribution to A_K over the investigated temperature range. This theoretical value was not used, however, as it was derived using a basis set that has been shown to be unreliable for estimating second hyperpolarizabilities for similar molecules.[7]

The Kerr first virial coefficients of pyridine were then analyzed using the equation

$$A_K T = (N_A/81\varepsilon_0 k)\Big\{\Big[(2/3)\mu\beta^K + (9/5)\alpha\alpha^0\kappa^2\Big] + (3/10k)\mu^2(\alpha_{zz} - \alpha)T^{-1}\Big\} \qquad (7.1)$$

and the data are graphed in Figure 7.2. Despite the scatter of the data points being larger than the statistical uncertainties, the line of best fit is reasonably well defined, with an uncertainty of ± 8% in the gradient Substitution of the γ^K value calculated by Keshari et al. into equation 6.2 decreases the gradient by only 0.2% and the value of α_{zz} by 0.03%.

Table 7.2 lists the electric properties of pyridine. The molecular axes are defined such that the z - axis is coincident with the C_2 axis and the dipole moment, the x - axis is

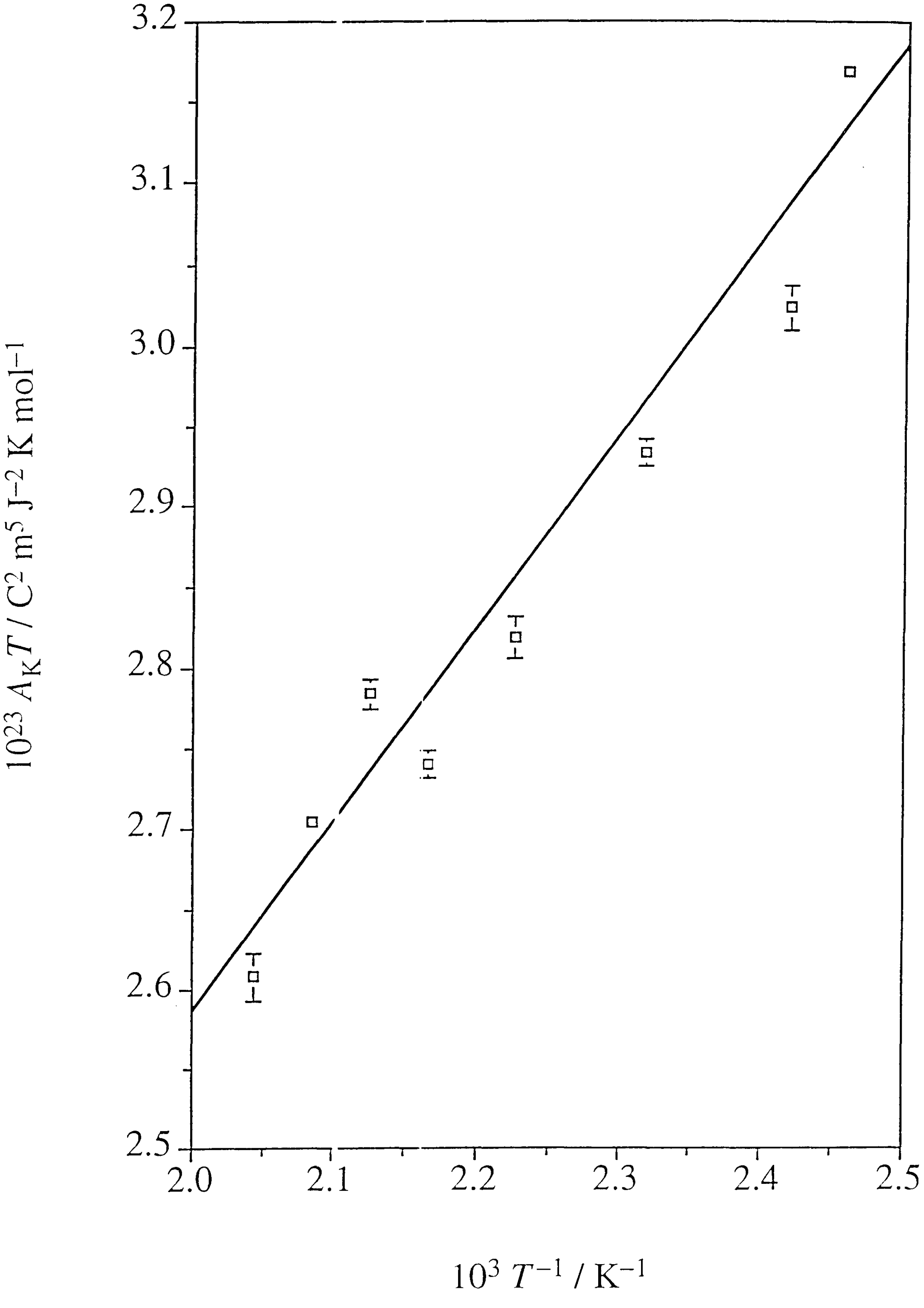

Figure 7.2 Analysis of the Kerr effect of pyridine.

Table 7.2 Analysis of the Kerr effect of pyridine at 632.8 nm

Property	Value
10^{21} slope / $C^2\ m^5\ J^{-2}\ K^{-1}\ mol^{-1}$ a)	12.0 ± 1.0
10^{24} intercept / $C^2\ m^5\ J^{-2}\ K^{-2}\ mol^{-1}$ a)	1.9 ± 2.1
$10^{40}\ \alpha$ / $C^2\ m^2\ J^{-1}$ b)	10.55 ± 0.11
$10^{40}\ \alpha^0$ / $C^2\ m^2\ J^{-1}$ c)	12.04 ± 0.60
$10^2\ \kappa^2$ d)	3.478 ± 0.034
$10^{30}\ \mu$ / C m c)	7.44 ± 0.07
$10^{60}\ \gamma^K$ / $C^4\ m^4\ J^{-3}$	≈ 0
$10^{40}\ (\alpha_{zz} - \alpha)$ / $C^2\ m^2\ J^{-1}$	1.64 ± 0.13
$10^{40}\ \alpha_{xx}$ / $C^2\ m^2\ J^{-1}$	12.83 ± 0.29
$10^{40}\ \alpha_{yy}$ / $C^2\ m^2\ J^{-1}$	6.63 ± 0.09
$10^{40}\ \alpha_{zz}$ / $C^2\ m^2\ J^{-1}$	12.19 ± 0.17
$10^{50}\ \beta^K$ / $C^3\ m^3\ J^{-2}$	-1.0 ± 0.7

a) From equation 7.1. b) Reference 18. c) Reference 19. d) Reference 22.

in the plane of the heterocyclic ring and the y - axis is orthogonal to the ring. A summary of the polarizabilities obtained from this and previous studies is given in Table 7.3. It has been generally recognized that $\alpha_{xx} > \alpha_{zz} > \alpha_{yy}$ for pyridine, and the same order is observed from this work. Although uncertainties were not quoted in many of the previous investigations, the limitations of the earlier studies and the assumptions used in their data analyses mean that their polarizabilities are considerably less precise and reliable than those determined in this work.

Despite the similarity in the measured Kerr constants, Stuart and Volkmann[8] deduced a somewhat greater anisotropy in the polarizability of the heterocyclic ring of pyridine than was found in this study. Le Fèvre and Le Fèvre[9] also obtained a larger in-plane polarizability anisotropy, but the contributions of the Kerr hyperpolarizabilities were unknown at the time of these earlier studies. Although this work also assumes γ^{K} to be negligible, Table 7.4 shows that the $\mu\beta^{\mathrm{K}}$ term is significant. Battaglia and Ritchie[10] were not able to separate the two in-plane polarizabilities and assumed that $\alpha_{xx} = \alpha_{zz}$ and $\beta^{\mathrm{K}} = 0$. The polarizabilities from the latter two studies were also determined from solution-phase measurements, and so are influenced by local-field effects.

Burnham and Gierke[11] combined the Kerr constant measured by Stuart and Volkmann with white light, the Rayleigh depolarization ratio and mean polarizability at 488.0 nm and $\beta(-2\omega;\omega,\omega)$, obtained from second harmonic generation measurements on pyridine solutions at 1060 nm.[15] to obtain polarizabilities that were in reasonable agreement with those from earlier studies. However, as will be discussed later in the chapter, this first hyperpolarizability is too small and the combination of polarizability data obtained at different wavelengths results in values that are unreliable.

Coonan[13] has determined a set of polarizabilities with large uncertainties from measurements of the temperature dependence of the Cotton-Mouton effect of pyridine at 632.8 nm. This imprecision was due to a combination of the practical limitations of the Cotton-Mouton effect, the unavoidably small temperature range used in Coonan's study and the relatively low precision of the magnetizabilities. The high inductance of the

Table 7.3 Investigations of the principal polarizabilities of pyridine [a)]

Year	Reference	Method	α_{xx}	α_{yy}	α_{zz}
1933	8	Vapour-phase Kerr effect using white light.	13.22	6.43	12.06
1955	9	Solution-phase Kerr effect at 589.3 nm.	12.68	6.12	11.57
1977	10	Solution-phase Kerr effect at 589.3 nm.	12.0	7.8	12.0
1980	11	${}_{\mathrm{m}}K_0$, ρ_0 and $\beta(-2\omega;\omega,\omega)$ at different wavelengths.	13.28	6.91	12.26
1990	12	SCF calculations (scaled to 632.8 nm).	13.02	6.57	12.23
1994	4	SDQ-MP4 calculations (static values).	12.71	6.77	11.99
1994	5	SCF calculations (static values).	12.06	6.63	11.31
1995	13	Vapour-phase Cotton-Mouton effect at 632.8 nm.	13.8 ± 1.2	7.0 ± 1.0	10.9 ± 1.6
1996	This work	Vapour-phase Kerr effect at 632.8 nm.	12.83 ± 0.29	6.63 ± 0.09	12.19 ± 0.17

a) Expressed in units of $10^{-40}\,\mathrm{C^2m^2J^{-1}}$.

iron-core magnet of the Cotton-Mouton effect apparatus used in Coonan's investigation makes modulation of the magnetic field very difficult, whereas modulation of the electric field is easily accomplished with the Kerr-effect apparatus. This leads to greater precision for the Kerr-effect measurements. Although the values reported by Coonan are as accurate as could be expected from the Cotton-Mouton effect study, they seem to be in less than satisfactory agreement with those obtained from this work.

There have also been several theoretical investigations of the polarizabilities of pyridine. Due to the size of this molecule, the highest levels of theory were precluded from use in these investigations. However, the results of Archibong and Thakkar[4] and Spackman[12] are in good agreement with those measured in this study.

Due to the large uncertainty of the intercept in Figure 7.2, the Kerr first hyperpolarizability is not well defined. However, these results do indicate that β^{K} for pyridine is negative in sign and of a similar magnitude to the β^{K} values of the dipolar fluorobenzenes in Chapter 6, the only other aromatic molecules for which this quantity has been measured. Although this is the first reported value of β^{K} for pyridine, Levine and Bethea[15] measured $\beta(-2\omega;\omega,\omega)=(-0.21\pm0.03)\times10^{-50}\,\mathrm{C}^3\,\mathrm{m}^3\,\mathrm{J}^{-2}$ at 1060 nm for liquid pyridine, using the same sign convention as this study. Despite the large uncertainty in β^{K}, it appears for pyridine that β^{K} is more negative than $\beta(-2\omega;\omega,\omega)$.

The individual contributions to the Kerr first virial coefficients of pyridine at 400 K and 500 K are listed in Table 7.4. The relative contributions at both temperatures display a remarkable similarity to those of the dipolar fluorobenzenes, described in Chapter 6, with the $\mu^2(\alpha_{zz}-\alpha)$ term being dominant and the $\alpha\alpha^0\kappa^2$ term being larger than the $\mu\beta^{\mathrm{K}}$ term, which makes a negative contribution to A_{K}. Although the $\mu\beta^{\mathrm{K}}$ term is the smallest of the measured contributions, it is still significant and must be included in an accurate analysis of the Kerr effect of pyridine. The value of γ^{K} calculated by Keshari et al.[7] makes only a very small contribution (0.2%) to the measured Kerr first virial coefficient of pyridine over the investigated temperature range. Therefore, the assumption that $\gamma^{\mathrm{K}}\approx 0$ has a negligible effect on the determination of the polarizabilities and β^{K} of pyridine.

Table 7.4 Contributions of individual terms to A_K for pyridine [a)]

Term	400 K	500 K
$(N_A/81\varepsilon_0)\gamma^K$	≈ 0	≈ 0
$(2N_A/243\varepsilon_0 kT)\mu\beta^K$	−7.3 (−9.2%)	−5.9 (−11.2%)
$(9N_A/405\varepsilon_0 kT)\alpha\alpha^0\kappa^2$	12.1 (15.2%)	9.7 (18.5%)
$\left(N_A/270\varepsilon_0 k^2T^2\right)\mu^2(\alpha_{zz} - \chi)$	74.9 (93.9%)	47.9 (91.5%)
A_K	79.8	52.4

a) Expressed in units of 10^{-27} C^2 m^5 J^{-2} mol^{-1}.

7.4 CONCLUSIONS

This study has resolved the uncertainty surrounding the polarizabilities of pyridine. The relative magnitudes of the polarizability components determined in this study are in agreement with earlier investigations. The accuracy of these Kerr-effect measurements, combined with the mean polarizability and depolarization ratio at the same wavelength, however, have resulted in the most reliable set of polarizabilities yet reported for this molecule. Although the Kerr first hyperpolarizability of pyridine was not determined to the same level of precision, it is in good agreement with those of other dipolar aromatic molecules.

7.5 REFERENCES

1 Schindler, M., *Magn. Res. Chem.*, **26**, 394 (1988).

2 Heitz, S., Weidauer, D. and Hese, A., *J. Chem. Phys.*, **95**, 7952 (1991).

3 Yang, W.-H. and Schatz, G.C., *J. Chem. Phys.*, **97**, 3831 (1992).

4 Archibong, E.F. and Thakkar, A.J., *Mol. Phys.*, **81**, 557 (1994).

5 Hinchliffe, A. and Soscún M, H.J., *J. Mol. Struct. (Theochem)*, **304**, 109 (1994).

6 Hinchliffe, A. and Soscún M, H.J., *J. Mol. Struct. (Theochem)*, **312**, 57 (1994).

7 Keshari, V., Wijekoon, W.M.K.P., Prasad, P.N. and Karna, S.P., *J. Phys. Chem.*, **99**, 9045 (1995).

8 Stuart, H.A. and Volkmann, H., *Ann. Phys.*, **18**, 21 (1933).

9 Le Fèvre, C.G. and Le Fèvre, R.J.W., *J. Chem. Soc.*, 2750 (1955).

10 Battaglia, M.R. and Ritchie, G.L.D., *J. Chem. Soc., Faraday Trans. 2*, 209 (1977).

11 Burnham, A.K. and Gierke, T.D., *J. Chem. Phys.*, **73**, 4822 (1980).

12 Spackman, M.A., unpublished results.

13 Coonan, M.H., *Ph.D. Thesis* (University of New England, 1995).

14 Flygare, W.H. and Benson, R.C., *Mol. Phys.*, **20**, 225 (1971).

15 Levine, B.F. and Bethea, C.G., *J. Chem. Phys.*, **63**, 2666 (1975).

16 Dymond, J.H. and Smith, E.B., *The Virial Coefficients of Pure Gases and Mixtures* (Clarendon Press, Oxford, 1980).

17 Hirschfelder, J.O., Curtiss, C.F. and Bird, R.B., *Molecular Theory of Gases and Liquids* (Wiley, New York, 1964).

18 Timmermans, J., *Physico-Chemical Constants of Pure Organic Compounds* (Elsevier, New York, 1950).

19 Buckingham, A.D., Chau, J.Y.H., Freeman, H.C., Le Fèvre, R.J.W., Narayana Rao, D.A.A.S. and Tardif, J. *J. Chem. Soc.*, 1405 (1956).

20 Gentle, I.R. and Ritchie, G.L.D., *J. Phys. Chem.*, **93**, 7740 (1989).

21 Halliburton, B.W., *B.Sc. Honours Thesis* (University of New England, 1988).

22 Keir, R.I., *Ph.D. Thesis* (University of New England, 1995).

CHAPTER 8 - KERR EFFECT, ANISOTROPIC POLARIZABILITY AND HYPERPOLARIZABILITIES OF FLUOROETHANE

8.1 INTRODUCTION

An extension of investigations of the halogenated methanes, discussed in Chapter 5, to the halogenated ethanes is an obvious next step in furthering understanding of the polarizabilities and hyperpolarizabilities of aliphatic molecules. Stuart and Volkmann[1] and Le Fèvre et al.[2,3,4] have measured the Kerr effects of several of the halogenated ethanes in the gas and solution phases, respectively. However, these earlier studies were unable fully to analyze the polarizabilities of these species, and did not investigate the Kerr effect of fluoroethane.

For molecules with C_s symmetry in their minimum-energy conformations, such as the halogenated ethanes, the direction of one of the principal axes of the polarizability does not coincide with the dipole moment. As discussed in Chapter 3, a combination of experiment and theory can be used to determine all four components of the polarizability for these species. Stankey[5] derived the polarizabilities of chloroethane and bromoethane from measurements of the temperature dependence of the vapour-phase Kerr effects of these compounds and ab initio calculations. A similar investigation of iodoethane was not possible, due to decomposition of the sample in the Kerr cell. The aim of this study was to measure the temperature dependence of the vapour-phase Kerr effect of fluoroethane, and to combine the results with ab initio calculations to determine the polarizabilities and hyperpolarizabilities of this molecule. Comparison with the results for chloroethane and bromoethane would then provide further information about the effects of halogen and methyl-group substitution on these properties.

8.2 EXPERIMENTAL

The sample of fluoroethane (Pfaltz and Bauer, > 99%) was used without further purification. Although fluoroethane is a gas at normal temperatures and pressures, the vapour pressures were kept low, due to the limited availability of sample. In order to compensate for this, and the small signals that were detected, Kerr effect measurements at each temperature were recorded at a larger number of pressures than normal.

Density second virial coefficients for fluoroethane were available only for the temperature range 290 - 310 K,[6] and the Stockmayer potential[7] was used to estimate the coefficients at higher temperatures. Keir[8] recently measured the mean polarizability of fluoroethane at 632.8 nm using the Rayleigh light-scattering apparatus, and an uncertainty of ± 1% was assigned to this value in the analysis of the Kerr effect results. The mean static polarizability was obtained from dielectric polarization measurements,[9] with an uncertainty of ± 5%, and the dipole moment of fluoroethane was measured by Hayashi et al.,[10] using Stark-effect spectroscopy. Table 8.1 lists the Kerr first and second virial coefficients measured for fluoroethane.

8.3 DISCUSSION

As fluoroethane has C_s symmetry in the minimum-energy staggered conformation,[10] the Kerr-effect results were analyzed in the manner described for methylamine and dimethylamine in Chapter 3. This required an estimate of the Kerr second hyperpolarizability and the fitting of the data to the equation

$$\begin{aligned}\left[A_{\mathrm{K}} - (N_{\mathrm{A}}/81\varepsilon_0)\gamma^{\mathrm{K}}\right]T = (N_{\mathrm{A}}/81\varepsilon_0 k)\Big\{&\left[(2/3)\mu\beta^{\mathrm{K}} + (9/5)\alpha\alpha^0\kappa^2\right] \\ &+ (3/10k)\mu^2(\alpha_{zz} - \alpha)T^{-1}\Big\}.\end{aligned} \qquad (8.1)$$

Buckingham et al.[11] have measured $\gamma^{\mathrm{K}} = (0.24 \pm 0.05)\times 10^{-60}$ C^4 m^4 J^{-3} for ethane at 632.8 nm and Buckingham and Orr[12] have determined that fluorine substitution in

Table 8.1 Kerr effect of fluoroethane at 632.8 nm

T / K	Number of Pressures	Pressure Range / kPa	$10^6 B$ [a)] / $m^3\ mol^{-1}$	$10^{27} A_K$ / $C^2\ m^5\ J^{-2}\ mol^{-1}$	$10^{30} B_K$ [b)] / $C^2\ m^8\ J^{-2}\ mol^{-2}$
296.3	14	40 - 119	−382	5.79 ± 0.02	9.0 ± 0.4
313.1	12	34 - 115	−332	5.58 ± 0.01	6.8 ± 0.2
330.0	13	35 - 107	−286	5.42 ± 0.02	5.4 ± 0.6
350.5	15	29 - 93	−243	5.01 ± 0.01	2.3 ± 0.3
372.9	15	33 - 99	−207	4.59 ± 0.01	0.3 ± 0.5
395.7	12	36 - 94	−178	4.22 ± 0.01	−2.2 ± 0.5
417.2	10	36 - 101	−156	3.82 ± 0.02	−1.3 ± 0.7
440.3	12	34 - 101	−136	3.50 ± 0.01	−0.6 ± 0.7
464.0	13	34 - 107	−120	3.21 ± 0.03	−1.1 ± 1.3
497.9	13	44 - 108	−103	3.06 ± 0.01	−6.8 ± 0.5

a) Density second virial coefficients from reference 6 and calculated values (see text). b) Calculated using $10^{40}\alpha / C^2\ m^2\ J^{-1} = 5.02 \pm 0.05$, from reference 8, $10^{40}\alpha^0 / C^2\ m^2\ J^{-1} = 5.52 \pm 0.28$, from reference 9, and $10^{30}\mu / C\,m = 6.461 \pm 0.023$, from reference 10.

methane decreases γ^{K} by $0.022\times10^{-60}\,C^4\,m^4\,J^{-3}$ at the same wavelength. As the investigations detailed in the preceding chapters of this thesis have verified that the Kerr second hyperpolarizability is approximately additive, γ^{K} for fluoroethane was estimated to be $0.22\times10^{-60}\,C^4\,m^4\,J^{-3}$ at 632.8 nm. Even though this value should be reasonably accurate, it was assigned an uncertainty of ± 100% for the purposes of the analysis of the Kerr-effect results.

The analysis is depicted in Figure 8.1. It is not known why the data point that corresponds to the Kerr first virial coefficient measured at the lowest temperature deviates so markedly from the line of best fit. The gradient, consequently, has an uncertainty of ± 18%, but this has very little influence on the precision of α_{zz}, however, as the quantity $\alpha_{zz}-\alpha$ is very small. There was insufficient sample to repeat the measurements at the lower temperatures. Stankey[5] reported the gradients of the corresponding plots for chloroethane and bromoethane to be one to two orders of magnitude larger than that found for fluoroethane in this work.

Ab initio calculations at the MP2 level were performed by Mr R.I. Keir[13] to determine the polarizabilities of fluoroethane at 632.8 nm. These calculations were made with the same 6-31G (+sd+sp) basis set and Hartree-Fock dispersion used by Spackman for the calculations on methylamine and dimethylamine reported in Chapter 3, and at the experimental geometry reported by Hayashi et al.[10] The angle between the principal- and natural-axis systems for the polarizability of fluoroethane was found to be 52.7°. A variation of 2° in θ was found to change α_{xx} and α_{yy} by approximately 1%, and a variation of 10° changes these components by 3.1% and 3.7%, respectively. The magnitudes of α_{xx} and α_{yy} are relatively insensitive to θ, because the polarizability of fluoroethane is not very anisotropic.

Figure 8.2 shows the orientations of the polarizability axes of fluoroethane, chloroethane and bromoethane. The orientations of the natural axes, with respect to the carbon - carbon and halogen - carbon bonds, and the angle between the two sets of axes are indicated for each molecule. The $xz\,/\,x'z'$ plane is coincident with the mirror plane of each molecule in its most stable conformation, and the y - axis is orthogonal to this

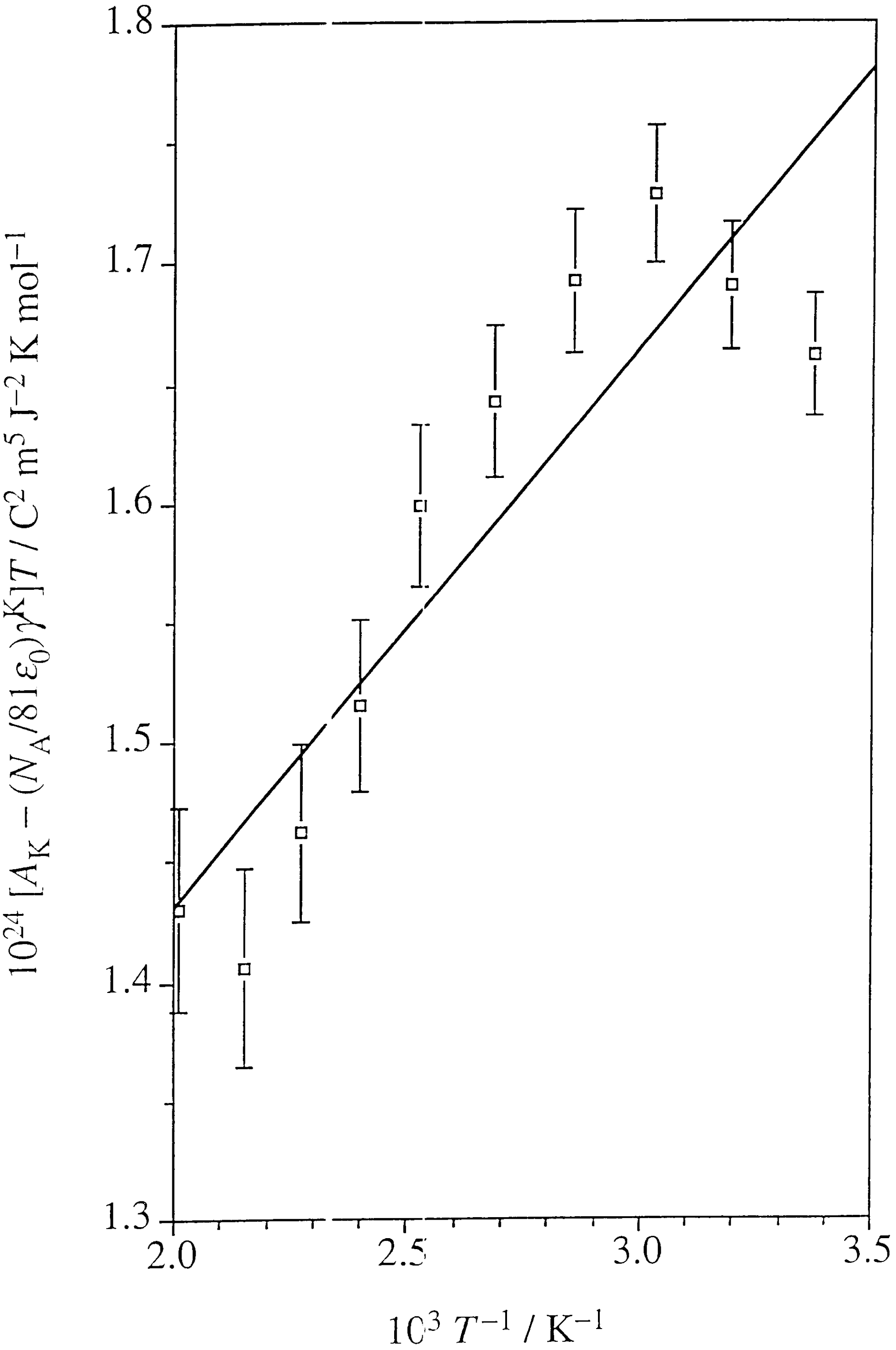

Figure 8.1 Analysis of the Kerr effect of fluoroethane.

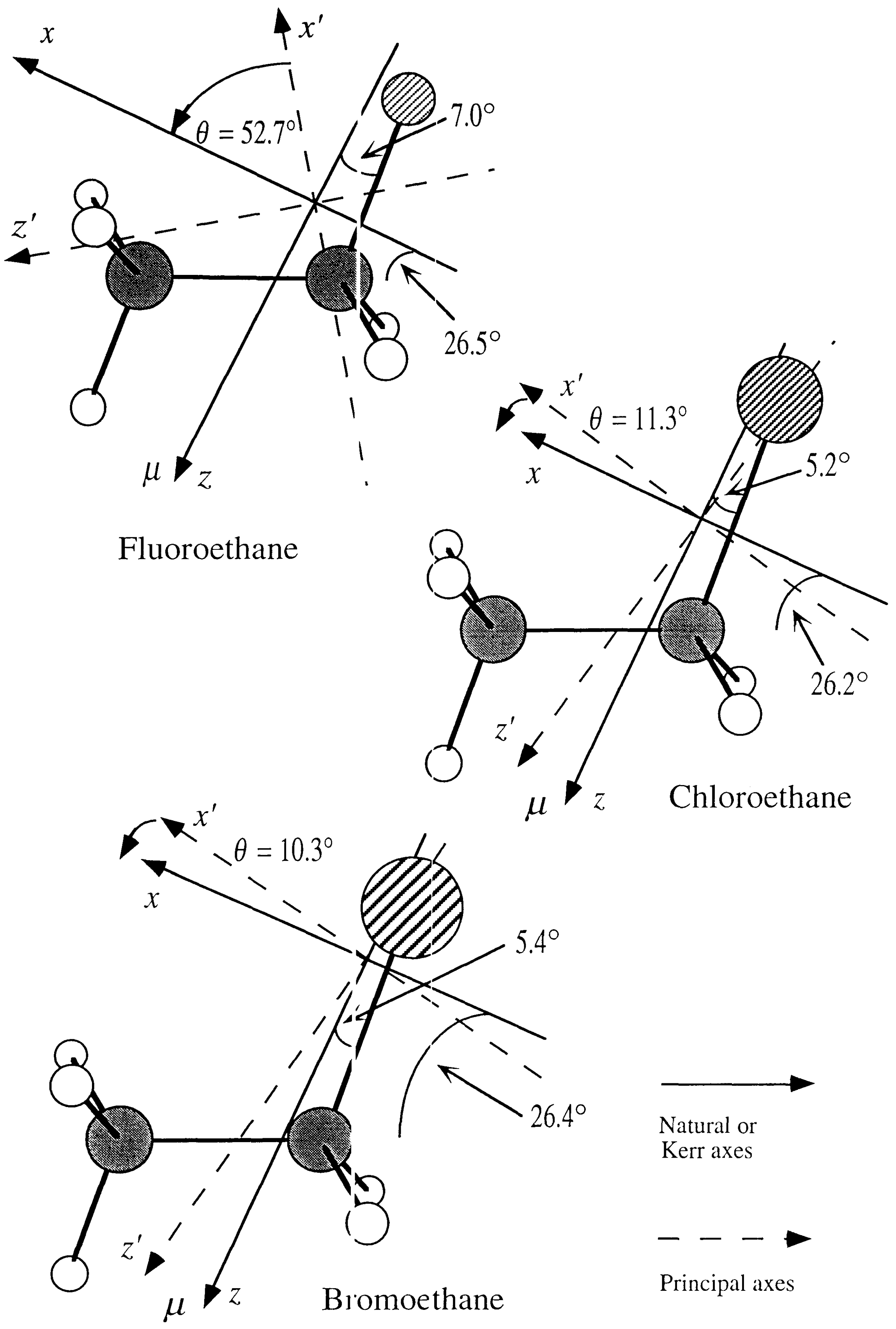

Figure 8.2 Orientation of the coordinate frames of the halogenoethanes.

plane. Hayashi et al.[10] found that the dipole moment of fluoroethane is oriented at an angle of 7.0° to the fluorine - carbon bond and the x - axis is oriented at 26.5° to the carbon - carbon bond.

As was discussed in Chapter 3, two sets of polarizabilities are obtained from the analysis of the Kerr-effect results for molecules with C_s symmetry in their minimum-energy conformations. Table 8.2 presents the two sets of polarizabilities for fluoroethane in comparison with the ab initio values calculated by Keir.[13] The polarizabilities in Set I were selected as being correct, due to their agreement with the theoretical values. The polarizabilities in Set II were obviously incorrect, as they predicted $\alpha_{yy} > \alpha_{xx}$. There is reasonable agreement between the mean polarizability measured using the Rayleigh light-scattering apparatus[8] and that predicted by additivity models, $\alpha = 4.84$ [14] and $4.91 \times 10^{-40}\,\mathrm{C^2\,m^2\,J^{-1}}$.[15] The electric properties of fluoroethane are summarized in Table 8.3.

Buckingham et al.[11] measured the Kerr effect of ethane at 632.8 nm and determined that the polarizability component perpendicular to the carbon - carbon bond,

Table 8.2 Comparison of experimental and theoretical polarizabilities of fluoroethane

	Set I	Set II	Ab initio a)
$10^{40}\alpha\,/\,\mathrm{C^2\,m^2\,J^{-1}}$	5.02 ± 0.05 b)	5.02 ± 0.05 b)	4.72
$10^{40}\alpha_{xx}\,/\,\mathrm{C^2\,m^2\,J^{-1}}$	5.30 ± 0.05	4.79 ± 0.15	4.90
$10^{40}\alpha_{yy}\,/\,\mathrm{C^2\,m^2\,J^{-1}}$	4.69 ± 0.15	5.21 ± 0.05	4.44
$10^{40}\alpha_{zz}\,/\,\mathrm{C^2\,m^2\,J^{-1}}$	5.06 ± 0.05	5.06 ± 0.05	4.81
$10^{40}\alpha_{xz}\,/\,\mathrm{C^2\,m^2\,J^{-1}}$	0.44 ± 0.12	−0.49 ± 0.12	0.16

a) Reference 13. b) Reference 8.

Table 8.3 Analysis of the Kerr effect of fluoroethane at 632.8 nm

Property	Value
10^{21} slope / $C^2 m^5 J^{-2} K^2 mol^{-1}$ a)	0.233 ± 0.041
10^{24} intercept / $C^2 m^5 J^{-2} K mol^{-1}$ a)	0.96 ± 0.11
10^{40} α / $C^2 m^2 J^{-1}$ b)	5.02 ± 0.05
10^{40} α^0 / $C^2 m^2 J^{-1}$ c)	5.52 ± 0.28
10^3 κ^2 b)	3.7948 ± 0.0033
10^{30} μ / C m d)	6.461 ± 0.023
10^{60} γ^K / $C^4 m^4 J^{-3}$	0.22
θ e)	52.7°
10^{40} α_{xx} / $C^2 m^2 J^{-1}$	5.30 ± 0.05
10^{40} α_{yy} / $C^2 m^2 J^{-1}$	4.69 ± 0.15
10^{40} α_{zz} / $C^2 m^2 J^{-1}$	5.06 ± 0.05
10^{40} α_{xz} / $C^2 m^2 J^{-1}$	0.44 ± 0.12
10^{50} β^K / $C^3 m^3 J^{-2}$	0.34 ± 0.04

a) From equation 8.1 b) Reference 8. c) Reference 9. d) Reference 10.

e) Reference 13.

α_{yy}, was equal to 4.68×10^{-40} C^2 m^2 J^{-1}. This value is virtually identical to that of the α_{yy} component for fluoroethane found from this study. As the y - axes of these two molecules are both perpendicular to the planes of symmetry, this verifies that replacement of hydrogen by fluorine in an aliphatic molecule has a negligible effect on the polarizability of the molecule perpendicular to the halogen - carbon bond. Stankey found that replacement of hydrogen by chlorine and bromine has a greater effect, with $\alpha_{yy} = (6.00 \pm 0.45) \times 10^{-40}$ C^2 m^2 J^{-1} for chloroethane and $(7.27 \pm 0.39) \times 10^{-40}$ C^2 m^2 J^{-1} for bromoethane.

It is not possible directly to compare the α_{xx} and α_{zz} components of fluoroethane with those of ethane, as the natural axes of these two compounds are not coincident. Similarly, the natural axes of chloroethane and bromoethane are not coincident with those of fluoroethane, or each other, and so their magnitudes also cannot be directly compared. However, a qualitative comparison can still be made. Stankey[5] found that $\alpha_{zz} > \alpha_{xx}$ for chloroethane and bromoethane, whereas $\alpha_{zz} < \alpha_{xx}$ for fluoroethane. Figure 8.2 shows that the z -axes of chloroethane and bromoethane are approximately parallel to the chlorine - carbon and bromine - carbon bonds, respectively. The dipole moment of chloroethane makes an angle of 5.2° with the chlorine - carbon bond, and the dipole moment of bromoethane makes an angle of 5.4° with the bromine - carbon bond.[10] As these bonds are far more polarizable than the carbon - carbon and hydrogen - carbon bonds,[14] α_{zz} is expected to be significantly larger than α_{xx} for chloroethane and bromoethane. The polarizabilities of the carbon - carbon, hydrogen - carbon and fluorine - carbon bonds are too similar to estimate the relative sizes of α_{xx} and α_{zz} for fluoroethane. It is, therefore, not surprising to find that they are similar for this molecule. The off-diagonal component of the polarizability of fluoroethane, $\alpha_{xz} = (0.44 \pm 0.12) \times 10^{-40}$ C^2 m^2 J^{-1}, is small and similar to the off-diagonal components for chloroethane and bromoethane, (0.27 ± 0.11) and $(0.52 \pm 0.15) \times 10^{-40}$ C^2 m^2 J^{-1}, respectively.

In the present work, Stankey's Kerr-effect measurements[5] were reanalyzed with revised estimates of the Kerr second hyperpolarizabilities to obtain the Kerr first hyperpolarizabilities of chloroethane and bromoethane. The values of $\gamma^K = 0.50$ and $0.76 \times 10^{-60}\ C^4\,m^4\,J^{-3}$ for chloroethane and bromoethane, respectively, were obtained in an identical manner to that described for fluoroethane from the Kerr second hyperpolarizabilities of ethane,[11] chloromethane[16] and bromomethane. Although these estimated γ^K values should be reliable and they make only a very small contribution to the Kerr constants of these molecules, as will be shown later, they were assigned uncertainties of ± 100% for the purposes of the reanalysis of Stankey's Kerr-effect data.

Mean static polarizabilities for chloroethane and bromoethane were obtained from dielectric polarization measurements,[9] and were assigned uncertainties of ± 5%. The Kerr first hyperpolarizabilities of chloroethane and bromoethane were found to be (0.48 ± 0.15) and $(0.8 \pm 0.3) \times 10^{-50}\ C^3\,m^3\,J^{-2}$, respectively. These are similar to the value of $(0.34 \pm 0.04) \times 10^{-50} C^3\,m^3\,J^{-2}$ for fluoroethane. Table 8.4 lists the Kerr first hyperpolarizabilities of the monohalogenated methanes and ethanes at 632.8 nm, with the value for bromomethane being taken from Chapter 5. Although further research is required conclusively to identify any trends, it appears that increasing the size of the halogen atom increases β^K for small halogenoalkanes, and that extension of the carbon chain also leads to β^K becoming larger and more positive.

Table 8.4 Kerr first hyperpolarizabilities of the halogenomethanes and halogenoethanes at 632.8 nm [a)]

	X = F	X = Cl	X = Br
CH_3X	−0.19 ± 0.15 [b)]	−0.1 ± 0.4 [c)]	0.5 ± 0.1
CH_3CH_2X	0.34 ± 0.04	0.48 ± 0.15 [d)]	0.8 ± 0.3 [d)]

a) Expressed in units of $10^{-50}\ C^3\,m^3\,J^{-2}$. b) References 12 and 16. c) Reference 17.

d) Reference 5, reanalyzed results.

The four contributions to the Kerr first virial coefficients of fluoro-, chloro- and bromo-ethane are listed in Table 8.5. It is obvious that the relative contributions of the four terms to A_K for chloroethane and bromoethane are almost identical. These contributions are very similar to those for bromomethane, given in Chapter 5. The $\mu^2(\alpha_{zz} - \alpha)$ term is dominant and the $\mu\beta^K$ term is larger than the $\alpha\alpha^0\kappa^2$ term, which is, in turn, larger than the γ^K term. For fluoroethane, however, the $\mu^2(\alpha_{zz} - \alpha)$ term makes a much smaller contribution, as $\alpha_{zz} - \alpha$ is very small, and the $\mu\beta^K$ term is largest. This large $\mu\beta^K$ contribution in fluoroethane leads to a more accurate determination of β^K for this molecule than for chloroethane or bromoethane.

Table 8.5 Contributions of individual terms to A_K of fluoroethane, chloroethane and bromoethane at 300 K [a)]

Term	CH_3CH_2F	CH_3CH_2Cl	CH_3CH_2Br
$(N_A/81\varepsilon_0)\gamma^K$	0.18 (2.9%)	0.4 (0.4%)	0.6 (0.5%)
$(2N_A/243\varepsilon_0 kT)\mu\beta^K$	2.98 (48.6%)	4.5 (4.6%)	7.1 (5.0%)
$(9N_A/405\varepsilon_0 kT)\alpha\alpha^0\kappa^2$	0.38 (6.2%)	2.0 (2.1%)	3.9 (2.7%)
$(N_A/270\varepsilon_0 k^2T^2)\mu^2(\alpha_{zz} - \alpha)$	2.59 (42.3%)	89.8 (92.8%)	130.5 (91.9%)
A_K	6.13	96.7	142.0

a) Expressed in units of 10^{-27} C^2 m^5 J^{-2} mol^{-1}.

Despite the small pressure ranges used for the Kerr effect measurements on fluoroethane, the Kerr second virial coefficients were measured to a reasonable level of precision. Table 8.1 shows that B_{K} for fluoroethane is positive at low temperatures, becomes zero at approximately 375 K and is negative at higher temperatures. These values are an order of magnitude larger than those of ethane at the same temperatures and are up to an order of magnitude smaller than those measured by Stankey[5] for chloroethane and bromoethane. Only the B_{K} values for fluoroethane show an obvious and systematic change in magnitude and sign with temperature.

8.4 CONCLUSIONS

This study has yielded reliable polarizabilities for fluoroethane, including the off-diagonal component. Although the polarizabilities of fluoroethane in the mirror plane of the molecule cannot be qualitatively compared with those of ethane, chloroethane or bromoethane, bond polarizabilities and the orientations of the respective dipole moments were used to explain their relative magnitudes. The Kerr first hyperpolarizability of fluoroethane was found to be in good agreement with those of the other halogenoethanes, and the effects of halogen and methyl-group substitution on β^{K} were explored.

8.5 REFERENCES

1 Stuart, H.A. and Volkmann, H., *Ann. Physik*, **18**, 121 (1933).

2 Le Fèvre, C.G., Le Fèvre, R.J.W. and Williams, A.J., *J. Chem. Soc.*, 4188 (1965).

3 Le Fèvre, R.J.W. and Orr, B J., *J. Chem. Soc.*, 5349 (1965).

4 Le Fèvre, R.J.W. and Orr, B J., *J. Chem. Soc. B*, 37 (1966).

5 Stankey, R., *M.Sc. Thesis* (University of New England, 1991).

6 Bignell, C.M. and Dunlop, P.J., *J. Chem. Phys.*, **98**, 4889 (1993).

7 Hirschfelder, J.O., Curtiss, C F. and Bird, R.B., *Molecular Theory of Gases and Liquids* (Wiley, New York, 1964).

8 Keir, R.I., *Ph.D. Thesis* (University of New England, 1995).

9 Maryott, A.A. and Buckley, F., *Table of Dielectric Constants and Electric Dipole Moments of Substances in the Gaseous State* (National Bureau of Standards, Washington D.C., 1953).

10 Hayashi, M., Fujitake, M., Inagusa, T. and Miyazaki, S., *J. Mol. Structure*, **216**, 9 (1990).

11 Buckingham, A.D., Bogaard, M.P., Dunmur, D.A., Hobbs, C.P. and Orr, B.J., *Trans. Faraday Soc.*, **60**, 1545 (1970).

12 Buckingham, A.D. and Orr, B.J., *Trans. Faraday Soc.*, **65**, 673 (1969).

13 Keir, R.I., unpublished results.

14 Miller, K.J., *J. Am. Chem. Soc.*, **112**, 8533 (1990).

15 Vogel, A., Cresswell, W., Jeffrey, G. and Leicester, I., *Chem. Industry*, 358 (1950).

16 Orr, B.J., *Hyperpolarizabilities of Halogenated Methane Molecules: A Critical Survey* in *Nonlinear Behaviour of Molecules, Atoms and Ions in Electric, Magnetic and Electromagnetic Fields* (L. Néel ed.), (Elsevier, Amsterdam, 1979).

17 Bogaard, M.P., Orr, B.J., Buckingham, A.D. and Ritchie, G.L.D., *J. Chem. Soc., Faraday Trans. 2*, **74**, 1573 (1978).

CHAPTER 9 - CONCLUSIONS

The preceding chapters of this thesis have detailed investigations into the Kerr effects of seventeen compounds, with the results being combined with those from Rayleigh light-scattering studies, ab initio calculations and other data in order to determine molecular polarizabilities and Kerr first and second hyperpolarizabilities. These systematic studies have allowed the electric properties of interest to be analyzed in terms of the molecular structure. The main conclusions drawn from these investigations are summarized in this chapter.

9.1 ELECTRIC POLARIZABILITIES

For those molecules with a permanent dipole moment and C_{2v} or higher symmetry, the polarizabilities were obtained from measurements of the density- and temperature dependence of the Kerr effect, the Rayleigh depolarization ratio and the mean polarizability. The Kerr effect has been further shown to be an excellent tool for deriving the polarizabilities of such species, due to the usual dominance of the $\mu^2(\alpha_{zz} - \alpha)$ contribution. Great care was taken to use data obtained at the optical frequency corresponding to a wavelength of 632.8 nm wherever possible, in order to avoid any errors due to dispersion The quadratic nature of the analysis gave rise to some possible ambiguity in the polarizabilities, but this was easily resolved in each case by intuitive arguments or comparison with theory. Several species with C_s symmetry were also investigated and the polarizabilities, including the small off-diagonal component, of these molecules were accurately resolved through a combination of experiment and theory. Although the polarizabilities of methylamine, dimethylamine and fluoroethane were reasonably insensitive in the angle, θ, between the principal polarizability axis and the dipole moment, this procedure promises to assist the full description of the polarizability tensors of an even wider range of molecules, which had previously been impossible.

The first experimental polarizabilities for methylamine, dimethylamine, dibromomethane, fluoroethane, 1,3-difluorobenzene and 1,2,3,5-tetrafluorobenzene have been presented in this thesis. It is, therefore, not possible to compare these with other experimental values. However, improvements in the apparatus and operating procedures have resulted in high levels of precision and reliability for all of the polarizabilities of the species that were investigated. Furthermore, the polarizabilities of the first four of the above compounds are in good to excellent agreement with theoretical values.

The first reported study of the temperature dependence of the Kerr effect of pyridine assisted the resolution of the long standing ambiguity of the magnitudes of the polarizabilities of this species. Nitrogen substitution into benzene was shown to reduce the polarizability in the direction of the dipole moment, and it would be of interest to further this study by investigating the polarizabilities of the diazines.

Measurements of the Kerr effects of the bromomethanes, in combination with previous studies on the fluoromethanes[1] and chloromethanes,[2] have resulted in the most comprehensive experimental investigation of the effects of halogen substitution on the polarizabilities yet reported. It is already well recognized that the mean polarizability and the magnitudes of the components increase as the size and number of the halogen atoms increase. In Chapter 5, this was first verified for the bromomethanes, and then the effects of halogen substitution on the relative contributions to the polarizability were explored. Bromine and chlorine substitution were shown to increase the anisotropy, relative to the mean polarizability, in a very similar manner. Fluorine substitution, however, induces very little anisotropy in the polarizability. This was rationalized in terms of the similarities in the geometries of analogous bromo- and chloro-methanes, and the fact that bromine - carbon and chlorine - carbon bonds are far more polarizable than fluorine - carbon and hydrogen - carbon bonds. The study of the halogenomethanes was extended to the halogenoethanes. Although the noncoincidence of the natural axes for the molecules in this series prevented a similar analysis of the relative contributions to the polarizability, bromine and chlorine substitution were again shown to have a similar influence on the polarizabilities, and much larger than that of fluorine.

For nondipolar molecules with C_{2v} or higher symmetry, the Kerr effect provides information on the static polarizability anisotropy and its relationship to the optical-frequency polarizability anisotropy. The substitution of two methyl groups into acetylene was found to increase the ratio $\Delta\alpha^0/\Delta\alpha$. This term was still less than unity for dimethylacetylene, and the imprecision of the value for acetylene[3] prevented a definitive comparison. It may be desirable to repeat the measurements on acetylene using the more accurate apparatus described in Chapter 2. Comparison of the static polarizability anisotropy for dimethylacetylene with the electronic contribution illustrated the errors in estimates of $\Delta\alpha^0$ that may be introduced by neglecting the vibrational contribution.

Fluorine substitution into benzene was found to increase the ratio $\Delta\alpha^0/\Delta\alpha$, but to have only a small effect on the principal polarizabilities themselves, which was also observed in earlier work.[4,5] A detailed analysis of the effects of functional-group substitution on the vibrational component of the static polarizability lay outside the scope of this research. However, the observation that fluorine substitution into aromatic molecules appears to enhance the vibrational contribution significantly more than the electronic contribution to $\Delta\alpha^0$ remains of interest.

9.2 KERR FIRST HYPERPOLARIZABILITIES

Accurate measurements of the temperature dependences of the Kerr effects allowed the determination of the Kerr first hyperpolarizabilities of all of the dipolar molecules; ammonia, methylamine, dimethylamine, trimethylamine, methylacetylene, bromomethane, dibromomethane, tribromomethane, 1,2-difluorobenzene, 1,3-

difluorobenzene, 1,2,3,5-tetrafluorobenzene, pyridine and fluoroethane. The generally small contribution of the $\mu\beta^K$ term to A_K, and the large uncertainties in the mean static polarizabilities, resulted in larger relative uncertainties for the Kerr first hyperpolarizabilities than the polarizabilities. These values for β^K, however, are still more precise and reliable than those generally reported for other molecules.[2,5,6]

No systematic variation was found to occur in β^K with functional-group substitution. This was as expected, because the experimental observable of the Kerr first hyperpolarizability transforms as a vector. The results do indicate, however, that β^K tends to be larger for aromatic molecules than for simple aliphatic molecules, and tends to become larger and more positive in sign with progressive halogen substitution and as the size of the halogen atoms increases.

9.3 KERR SECOND HYPERPOLARIZABILITIES

It is difficult to obtain precise values of the Kerr second hyperpolarizabilities of dipolar, and even many nondipolar, molecules, due to the small contribution of this term to A_K. However, this work has shown that careful measurements of the temperature dependence of the Kerr effect can result in Kerr second hyperpolarizabilities accurate to within ± 10%, even for polyatomic molecules. Kerr second hyperpolarizabilities were measured for ammonia, trimethylamine, methylacetylene, dimethylacetylene, bromomethane, tribromomethane, tetrabromomethane, 1,4-difluorobenzene and 1,2,4,5-tetrafluorobenzene. The investigations of the methylacetylenes, bromomethanes and fluorobenzenes supported the applicability of the bond additivity approximation.[1,4] This allows reasonable values of γ^K to be estimated for many molecules where it cannot be accurately measured. Care must be taken when comparing both first and second hyperpolarizabilities relating to different nonlinear optical processes and different physical states. In the past, Kerr effect data have been interpreted using hyperpolarizabilities obtained from other nonlinear optical effects.[6,7,8] The results presented in this thesis clearly demonstrate the errors that may arise in this procedure, particularly when the effects of dispersion are not taken into account.

9.4 KERR SECOND VIRIAL COEFFICIENTS

The measurement of Kerr second virial coefficients was a secondary aim of this project. It was possible to carry out only limited measurements of the density dependence of the Kerr effects for the majority of species investigated in this work, due to their low volatilities. As a result, the values of B_K were less reliable than the corresponding values of A_K in each case. No examination of the density dependence of the Kerr effects of tribromomethane and tetrabromomethane was possible, due to the low vapour pressures used. The values of B_K determined for the fluorobenzenes and pyridine are also uncertain. However, the measurement of Kerr second virial coefficients of polyatomic molecules is a very demanding task, and this work presents the first reported values of B_K for ammonia, methylamine, dimethylamine, trimethylamine, methylacetylene, dimethylacetylene, bromomethane, dibromomethane, 1,2-difluorobenzene, 1,3-difluorobenzene, 1,4-difluorobenzene, 1,2,3,5-tetrafluorobenzene, 1,2,4,5-tetrafluorobenzene, pyridine and fluoroethane. Accurate and reliable values of B_K were obtained for several of these compounds, and those of ammonia were shown to be in excellent agreement with values predicted by the collision-induced polarizability model,[9] at least at high temperatures. The divergence between theory and experiment at lower temperatures requires further investigation.

This work has confirmed that the temperature dependence of the Kerr effect of gases and vapours is a very important, and widely applicable, technique for the determination of electric properties of free molecules. It is clear that systematic studies of the effects of functional-group substitution on the polarizabilities and hyperpolarizabilities, of the type described in this thesis, provide considerable insight into the natures of these important properties.

9.5 REFERENCES

1 Buckingham, A.D. and Orr, B.J., *Trans. Faraday Soc.*, **65**, 673 (1969).

2 Bogaard, M.P., Orr, B.J., Buckingham, A.D. and Ritchie, G.L.D., *J. Chem. Soc., Faraday Trans. 2*, **74**, 1573 (1978).

3 Buckingham, A.D., Bogaard, M.P., Dunmur, D.A., Hobbs, C.P. and Orr, B.J., *Trans. Faraday Soc.*, **60**, 1548 (1970).

4 Gentle, I.R. and Ritchie, G.L.D., *J. Phys. Chem.*, **93**, 7740 (1989).

5 Gentle, I.R., Hesling, M.R. and Ritchie, G.L.D., *J. Phys. Chem.*, **94**, 1844 (1990).

6 Stankey, R., *M.Sc. Thesis* University of New England, 1991).

7 Burnham, A.K., Buxton, L.W. and Flygare, W.H., *J. Chem. Phys.*, **67**, 4990 (1977).

8 Burnham, A.K. and Gierke, T.D., *J. Chem. Phys.*, **73**, 4822 (1980).

9 Buckingham, A.D., Galwas, P.A. and Liu Fan-Chen, *J. Mol. Struct.*, **100**, 3 (1983).